

# Strain-specific alterations in gut microbiome and host immune responses elicited by *Bifidobacterium pseudolongum*

**Bing Ma** (✉ [bma@som.umaryland.edu](mailto:bma@som.umaryland.edu))

Institute of Genome Sciences, University of Maryland School of Medicine

**Samuel J. Gavzy**

Department of Surgery University of Maryland Medical Center

**Vikas Saxena**

Center for Vascular and Inflammatory Diseases, University of Maryland School of Medicine

**Yang Song**

Institute of Genome Sciences, University of Maryland School of Medicine

**Wenji Piao**

Center for Vascular and Inflammatory Diseases, University of Maryland School of Medicine

**Hnin Wai Lwin**

Institute of Genome Sciences, University of Maryland School of Medicine

**Ram Lakhan**

Center for Vascular and Inflammatory Diseases, University of Maryland School of Medicine

**Jegan Lyyathurai**

Center for Vascular and Inflammatory Diseases, University of Maryland School of Medicine

**Lushen Li**

Center for Vascular and Inflammatory Diseases, University of Maryland School of Medicine

**Michael France**

Institute of Genome Sciences, University of Maryland School of Medicine

**Christina Paluskievicz**

Center for Vascular and Inflammatory Diseases, University of Maryland School of Medicine

**Marina WillsonShirkey**

Center for Vascular and Inflammatory Diseases, University of Maryland School of Medicine

**Lauren Hittle**

Institute of Genome Sciences, University of Maryland School of Medicine

**Arshi Munawwar**

Institute of Human Virology, University of Maryland School of Medicine

**Emmanuel F. Mongodin**

Institute of Genome Sciences, University of Maryland School of Medicine

**Jonathan S. Bromberg**

## Research Article

**Keywords:** Bifidobacterium, strain-specificity, RNA-seq, 28 live biotherapeutics, gut microbiome, immunomodulation

**Posted Date:** March 18th, 2022

**DOI:** <https://doi.org/10.21203/rs.3.rs-1458908/v1>

**License:**   This work is licensed under a Creative Commons Attribution 4.0 International License.

[Read Full License](#)

---

3 **Strain-specific alterations in gut microbiome and host immune responses**  
4 **elicited by *Bifidobacterium pseudolongum***

5  
6  
7 Bing Ma<sup>1,2\*</sup>, Samuel J. Gavzy<sup>3,4</sup>, Vikas Saxena<sup>4</sup>, Yang Song<sup>1</sup>, Wenji Piao<sup>4</sup>, Hnin Wai  
8 Lwin<sup>1</sup>, Ram Lakhan<sup>4</sup>, Jegan Lyyathurai<sup>4</sup>, Lushen Li<sup>4</sup>, Michael France<sup>1,2</sup>, Christina  
9 Paluskievicz<sup>4</sup>, Marina WillsonShirkey<sup>4</sup>, Lauren Hittle<sup>1</sup>, Arshi Munawwar<sup>5</sup>, Emmanuel F.  
10 Mongodin<sup>1,2,#</sup>, Jonathan S. Bromberg<sup>2,3,4\*</sup>

11  
12 <sup>1</sup>Institute of Genome Sciences, University of Maryland School of Medicine, Baltimore,  
13 MD 21201, United States; <sup>2</sup>Department of Microbiology and Immunology, University of  
14 Maryland School of Medicine, Baltimore, MD 21201, United States; <sup>3</sup>Department of  
15 Surgery University of Maryland Medical Center, Baltimore, MD 21201, United States;  
16 <sup>4</sup>Center for Vascular and Inflammatory Diseases, University of Maryland School of  
17 Medicine, Baltimore, Maryland, Maryland, 21201, United States; <sup>5</sup>Institute of Human  
18 Virology, University of Maryland School of Medicine, Baltimore, Maryland, Maryland,  
19 21201, United States

20  
21 # Current affiliation: Division of Lung Diseases, National Heart, Lung, and Blood  
22 Institute (NHLBI), National Institutes of Health (NIH), Bethesda, Maryland, USA

23  
24 \* Corresponding authors

25 Bing Ma: [bma@som.umaryland.edu](mailto:bma@som.umaryland.edu)

26 Jonathan S. Bromberg: [JBromberg@som.umaryland.edu](mailto:JBromberg@som.umaryland.edu)

- 28 **Key words:** *Bifidobacterium*, strain-specificity, RNA-seq, live biotherapeutics, gut
- 29 microbiome, immunomodulation

30 **ABSTRACT**

31 **Background:**

32           The beneficial effects attributed to *Bifidobacterium* are thought to arise from their  
33 host immunomodulatory capabilities, which are likely to be species- and even strain-  
34 specific. However, their strain-specificity in direct and indirect immune modulation  
35 remain largely uncharacterized.

36 **Results:**

37           We have shown that *B. pseudolongum* UMB-MBP-01, a murine isolate, is  
38 capable of suppressing inflammation and reducing fibrosis *in vivo*. To ascertain the  
39 mechanism driving this activity and to determine if it is specific to UMB-MBP-01, we  
40 compared it to *B. pseudolongum* type strain ATCC25526 of porcine origin using a  
41 combination of *in vitro* and *in vivo* experimentation and comparative genomics  
42 approaches. Despite many shared features, we demonstrate that these two strains  
43 possess distinct genetic repertoires in carbohydrate assimilation, differential activation  
44 signatures and cytokine responses in innate immune cells, and differential effects on  
45 lymph node morphology with unique local and systemic leukocyte distribution.  
46 Importantly, the administration of each *B. pseudolongum* strain resulted in major  
47 divergence in the structure, composition, and function of gut microbiota. This was  
48 accompanied by markedly different changes in intestinal transcriptional activities,  
49 suggesting strain-specific modulation of the endogenous gut microbiota as a key to host  
50 responses of immune modulation and changes in intestinal *B. pseudolongum* strains.

51 **Conclusion:**

52           Our study demonstrated a single probiotic bacterial strain can influence local,  
53 regional, and systemic immunity through both innate and adaptive pathways in a strain-  
54 specific manner. It highlights the importance to investigate both the endogenous gut  
55 microbiome in response to prophylactic supplementation strains and the intestinal  
56 responses, and advances our understanding of the mechanisms which drive the strain-  
57 specific association between prophylactic *Bifidobacterium* and health benefit.

## 58 **Introduction**

59 *Bifidobacterium* spp. are naturally occurring residents within the gastrointestinal  
60 (GI) tract of mammals and are typically considered beneficial [1, 2]. Due to their  
61 purported health-promoting properties, *Bifidobacterium* spp. have been incorporated  
62 into many live biotherapeutic (LBP) prophylactic formulations, mostly known for  
63 applications in alleviating intestinal inflammatory conditions [3-7]. The potential  
64 mechanisms underlying the health benefits of *Bifidobacterium* include the suppression  
65 of growth of gut pathogens [8, 9], capabilities to alter gut metabolism and to enhance  
66 epithelial barrier function [10, 11], and anti-inflammatory modulation of host immunity  
67 [12-15]. In particular, their immunomodulatory properties are not limited to the direct  
68 effects on GI tissues, but also indirect effects enacted through their influence on the gut  
69 microbiota [16]. *Bifidobacterium* spp. are known to participate in mutualistic interactions  
70 with endogenous intestinal microorganisms that can subsequently evoke both  
71 immediate as well as delayed immune responses [17, 18]. However, the cellular and  
72 molecular underpinnings *Bifidobacterium's* biotherapeutic effects remain unclear with  
73 contradictory findings reported [19]. Fundamentally important questions such as what  
74 specific mechanisms through which they exert immunomodulatory effects, to what  
75 extent the interactions with the gut microorganisms affect the immune responses, and  
76 what are the roles of elicited intestinal responses in these processes remain  
77 outstanding.

78 The immunomodulatory properties of individual *Bifidobacterium* spp. are strain-  
79 dependent, despite similar effects produced by closely related strains (i.e., alleviation of  
80 lactose intolerance or improved host antimicrobial activity) [20-22]. In fact,

81 immunomodulatory effects are independent of microbial phylogeny [20]. Recent  
82 investigations suggested that differences in cell wall composition and structure might be  
83 responsible for strain-specific immunomodulatory effects [23]. Microorganism-  
84 associated molecular patterns (MAMPs) possess variable biochemistry, even between  
85 strains, serving as microbial stimuli that orchestrate molecular cascades in the host  
86 immune response and mucosal homeostasis [24-26]. Exopolysaccharide (EPS) and pili  
87 may play a role in *Bifidobacterium*'s strain-specific pro-homeostatic immunomodulation  
88 [27, 28]. Other molecular mechanisms such as lipoteichoic acid and specific metabolites  
89 such as acetate could also contribute to strain-specific immunity [26, 29, 30].  
90 Comparisons of the immunomodulatory properties of closely related strains can be  
91 leveraged to identify which are strain-specific and to characterize the microbial  
92 determinants of specific host responses, which will provide the basis to rationally hone  
93 biotherapeutics for prophylactic applications [15, 31, 32].

94         We previously showed, using a major histocompatibility complex (MHC)-  
95 mismatched murine cardiac transplant model, that fecal microbiota transfer (FMT)  
96 caused shifts in the gut microbiota which profoundly influenced allograft outcomes [33].  
97 FMT using stool samples from healthy pregnant mice (immune suppressed) resulted in  
98 improved long-term allograft survival and prevented inflammation and fibrosis in grafts,  
99 as compared to FMT using stool samples from colitic or nonpregnant control mice [33].  
100 *B. pseudolongum* was revealed as a microbial biomarker for the pregnant mouse gut  
101 microbiota, from which we subsequently isolated and sequenced UMB-MBP-01 [34].  
102 Importantly, gavage with UMB-MBP-01 alone reproduced the same improved graft  
103 outcomes as FMT using whole stool of pregnant mice, implicating this strain as one of

104 the main responsible microbes [33]. Thus, the murine tropic strain UMB-MBP-01 may  
105 serve as a model organism to investigate the mechanisms of microbe-driven  
106 immunomodulation.

107 In this study, we performed a genome-wide comparison of UMB-MBP-01 to all  
108 other *B. pseudolongum* genomes, including three additional *B. pseudolongum* strains  
109 (E, EM10, EM13) isolated from the same feces sample of a pregnant mouse, as well as  
110 to the porcine tropic type strain ATCC25526, in order to investigate the genetic  
111 attributes underlying the immunomodulatory properties. Further, we revealed distinct  
112 effects on local and systemic immunity induced by UMB-MBP-01 and ATCC25526,  
113 using both *in vitro* and *in vivo* approaches. Importantly, the oral administration of the two  
114 *B. pseudolongum* strains resulted in profound alterations in composition, structure and  
115 function of the murine gut microbiome, accompanied with markedly different intestinal  
116 transcriptome activities. These observations suggest that modulation of the endogenous  
117 gut microbiome is a key element of *Bifidobacterium* immunomodulatory attributes. A  
118 deeper understanding of the strain specificity and mechanisms of action through which  
119 specific strains regulate host responses will facilitate the clinical translation of live  
120 therapeutics and the development of potential immunomodulatory therapy targets.

## 121 **Results**

### 122 High genome plasticity of *B. pseudolongum* reflects strong host adaptability

123           The pangenome of *B. pseudolongum* was constructed using 79 strains including  
124 the 4 strains sequenced as part of this study (**Supplemental Table 1A**). Homologous  
125 gene clusters (HGCs) were identified in this set of genomes based on all-versus-all  
126 sequence similarity (**Supplemental Table 1B**). A total of 4,321 *B. pseudolongum* HGCs  
127 were revealed, among which 31.7% were core (present in almost all strains), 57.0%  
128 were dispensable (singleton or present in very few genomes), and the remaining 11.3%  
129 were considered accessory. *B. pseudolongum* demonstrated a smaller pangenome size  
130 that was 87.8% of *B. breve* and 59.5% of *B. longum* pangenomes (**Supplemental**  
131 **Figure 1**). *B. pseudolongum* had the fewest number of conserved HGCs (N=1,370) but  
132 the largest proportion of dispensable pangenome (57.0%) compared to the two other  
133 *Bifidobacterium* species *B. longum* and *B. breve* that were both human-associated. This  
134 disproportionally large dispensable pangenome may be indicative of strong niche  
135 adaptation capabilities of *B. pseudolongum*, reflecting its broad host range, being widely  
136 distributed among mammals [35].

137           Whole genome sequencing was performed on three *B. pseudolongum* strains (E,  
138 EM10, and EM13) isolated from the same pregnant mice feces as UMB-MBP-01  
139 (sequencing statistics in **Supplemental Table 2A**). Comparison among the four murine  
140 strains revealed 1,520 shared coding DNA sequence (CDS), which comprised 97.2% of  
141 UMB-MBP-01 coding genes (**Supplemental Table 1C**). 107 CDS were conserved in at  
142 least two but not in all four genomes, and 37 CDS were strain-specific. Most of these  
143 genes had unknown functions, and those with known functions related to bacteriophage

144 assembly and function (i.e., capsid protein, integrase, transposes, bacteriophage  
145 replication gene, cell lysis protein, microvirus H protein) or carbohydrate hydrolysis and  
146 transport (glycosyl hydrolases, ABC transporter permease). On the other hand,  
147 comparison between UMB-MBP-01 and ATCC25526 revealed 1,351 shared CDS  
148 (86.4% of UMB-MBP-01 coding genes), and 157 genes that belonged to one strain but  
149 not the other (**Supplemental Table 1D**). Interestingly, most of these strain-specific  
150 genes also belonged to the categories of bacteriophage assembly and functions as well  
151 as carbohydrate hydrolysis and transport, in addition to genes with unknown function.  
152 Together these data suggested bacteriophage-mediated transduction was a major  
153 contributor to dissemination of carbohydrate metabolism capabilities, potentially through  
154 horizontal gene transfer among closely related murine-derived strains, as well as more  
155 distantly related *B. pseudolongum* strains.

156         Whole genome Average Nucleotide Identity (ANI) clustering suggested two  
157 subspecies, *B. pseudolongum* subsp. *pseudolongum* clade that contained ATCC25526,  
158 and *B. pseudolongum* subsp. *globosum* clusters that had three distinct clades I-III  
159 (**Figure 1**). Subspecies *globosum* clade III had the largest number of coding genes  
160 (1,642 $\pm$ 70) among all clades and contained UMB-MBP-01 and the three isolates from  
161 the source stools of pregnant mice. The subspecies *pseudolongum* clade had the  
162 smallest number of coding genes among all clades (1,519 $\pm$ 35.6). Overall, 1,599 HGCs  
163 accounted for 37.0% of *B. pseudolongum* pangenome were identified as clade-specific  
164 (>90% genes belonging to the same clade), and the majority originated from *globosum*  
165 clade III (N=648), while clade *pseudolongum* provided the fewest (N=130). The large  
166 number of clade-specific genes found in *globosum* clade III genomes suggested a high

167 degree of genome plasticity to facilitate adaptation to cope with environmental  
168 heterogeneity. Further functional enrichment analyses revealed *globosum* cluster III-  
169 specific HGCs were mostly involved in periplasmic transport systems, permeases and  
170 glycoside hydrolases (GHs), particularly the families GH29 ( $\alpha$ -L-fucosidase), GH3 ( $\beta$ -  
171 glucosidase) and GH31 ( $\alpha$ -glucosidase) (**Supplemental Table 1E**). No GH families  
172 were enriched in any of the other clades. Together, UMB-MBP-01 and ATCC25526  
173 belonged to two different subspecies, each of which comprises considerable genetic  
174 variation. The genome of UMB-MBP-01 contained more clade-specific genes and was  
175 enriched for genetic features in carbohydrate metabolism to assimilate greater varieties  
176 of glycans, presumably facilitating its niche adaptive capabilities in the glycan-rich gut  
177 environment.

#### 178 Specialized carbohydrate metabolizing capabilities of UMB-MBP-01 and ATCC25526

179 The abundance of *Bifidobacterium* glycolytic features is reflective of their  
180 metabolic adaptation to the complex carbohydrate-rich GI tract [36, 37]. We performed  
181 *in silico* prediction of the carbohydrate fermentation capabilities to comprehensively  
182 investigate glycan-assimilation capabilities for all 79 *B. pseudolongum* genomes, using  
183 with the Carbohydrate-Active enZYmes Database (CAZy) database [38]. This analysis  
184 revealed 236 genes of *B. pseudolongum* pangenome encoding predicted carbohydrate-  
185 active enzymes from 34 glycosyl hydrolase families, 14 glycosyl transferase families  
186 and eight carbohydrate esterase families (**Supplemental Table 4A**). Only 33.5% of the  
187 carbohydrate-active enzyme coding genes belonged to the core pangenome. Core GHs  
188 included those mostly responsible for the breakdown of plant-derived polysaccharides  
189 (*i.e.*, starch) and a wide range of other carbohydrates, such as GH13 (glycosidase),

190 GH77 ( $\alpha$ -amylase), GH43 ( $\beta$ -xylosidase), GH36 ( $\alpha$ -galactosidase), GH2 ( $\beta$ -  
191 galactosidase), GH3, and GH6 (cellobiohydrolases). Notably, GH13 is the enzyme  
192 family known to be most commonly found in *Bifidobacterium* genomes and active on a  
193 wide range of carbohydrates including the plant-derived starch and the related  
194 substrates of trehalose, stachyose, raffinose, and melibiose [37, 39]. Conversely, 47.9%  
195 of the identified carbohydrate-active enzymes genes were found in the dispensable  
196 pangenome. The *globosum* clade II (N=72) and III (N=58) encoded most of these  
197 enzymes, while the *pseudolongum* clade encoded the least (N=13). These results  
198 demonstrated the highly specialized carbohydrate assimilation gene repertoires of  
199 different strains, particularly in *globosum* clade II and III.

200       Using UMB-MBP-01 as the reference for all other *B. pseudolongum* strains, both  
201 conserved and specific glycohydrolases capabilities were revealed (**Supplemental**  
202 **Figure 2, Supplemental Table 1F, 4B**). Interestingly, the clusters based on GH are  
203 mostly in agreement with the clades generated based on ANI, suggesting distinct  
204 carbohydrates assimilation capabilities of different *B. pseudolongum* clades. GH29,  
205 GH31, GH42 ( $\beta$ -galactosidase), and ABC-type polysaccharide transport permease  
206 genes were most prevalent in *globosum* clade III that contained UMB-MBP-01. Further,  
207 GH36, GH2, and GH94 (cellobiose phosphorylase) were found absent in subspecies  
208 *pseudolongum* clade but prevalent in *globosum* clade III. In particular, an uncommon  
209 GH23 family (peptidoglycan lysases) was only observed in UMB-MBP-01 and the three  
210 other isolates from the pregnant mouse. Overall UMB-MBP-01 and ATCC25526 share  
211 some enzymatic capabilities in metabolizing dietary polysaccharides and host-derived  
212 glycogens, while also having specialized glycohydrolases genes.

213 We further characterize the carbohydrate utilization capabilities of UMB-MBP-01  
214 and ATCC25526 using anaerobic microplates pre-coated with various carbon sources.  
215 Out of the 95 carbon sources tested, the two strains demonstrated the same capabilities  
216 on 86 (90.5%) (**Supplemental Table 3**), including key carbon sources N-acetyl-D-  
217 glucosamine, D-fructose, L-fucose,  $\alpha$ -D-glucose, glucose-6-phosphate, maltose,  
218 maltotriose, D-mannose, D-sorbitol, and pyruvic acid. Two relatively uncommon sugars  
219 D-melibiose and D-raffinose could be metabolized by ATCC25526 but not UMB-MBP-  
220 01. On the other hand, D-galactose, D-gluconic acid, D-glucosaminic acid, glycerol, D-  
221 mannitol,  $\alpha$ -ketovaleric acid, and D, L-lactic acid were uniquely metabolized by UMB-  
222 MBP-01. This result is in principle in an agreement of the specific GH families  
223 predicated *in silico*. Together these data indicated a wide range of carbohydrate  
224 metabolizing capabilities ranging from dietary to host-derived glycans for both strains,  
225 while UMB-MBP-01 had specialized capabilities to metabolize galacto-oligosaccharides.

226 We sought to characterize the secretome of *B. pseudolongum* by examining  
227 protein localization based on the presence of a signal peptide [40]. Proteins which are  
228 secreted extracellularly have the potential to directly interact with the other gut  
229 microorganisms and with host tissues [27, 41] (**Supplemental Table 5A**). Overall, the  
230 sec-dependent secretion machinery, but not the twin-arginine (Tat) system, was  
231 conserved in all *B. pseudolongum* strains, indicating protein translocation function was  
232 conserved but likely occurs only in the unfolded state [42]. Secreted proteins were more  
233 likely to be part of the dispensable genome (73% of secreted proteins versus 53% of  
234 cytoplasmic proteins; **Supplemental Table 5B**), indicating a high degree of diversity in  
235 the secretome among strains of *B. pseudolongum*. Proteins which were predicted to be

236 extracellularly secreted include solute-binding proteins of ABC transporter systems,  
237 amidases related to the peptidoglycan hydrolysis, glycosyl hydrolases, cell surface  
238 proteins that make up pilus subunits, and cell wall-degrading peptidases. Interestingly,  
239 the secretome of the clade containing ATCC25526 was enriched for collagen adhesion  
240 proteins (**Supplemental Table 5C**) but lacked multiple secreted GH25 extracellular  
241 proteins. These proteins are prevalent in the clade which includes UMB-MBP-01 and  
242 are involved in the binding and hydrolysis of peptidoglycan (**Supplemental Table 5D**).  
243 As peptidoglycan components were implicated in important aspects of mucosal  
244 immunological signaling [43], this may contribute to varied immunomodulatory  
245 capabilities between UMB-MBP-01 and ATCC25526.

246 Differential activation and cytokine responses in dendritic cells and macrophages  
247 induced by *B. pseudolongum* strains ATCC25526 and UMB-MBP-01

248 To understand the immunomodulatory impact of the two *B. pseudolongum*  
249 strains, bone marrow derived dendritic cells (BMDC) and peritoneal macrophages (MΦ)  
250 were treated with UV-killed whole bacteria (cells) or isolated *Bifidobacterium*  
251 exopolysaccharide (EPS). We first examined the effect of these treatments on  
252 expression of costimulatory receptors. For BMDCs, treatment with either *B.*  
253 *pseudolongum* strain stimulated increased CD40 and CD86 expression, although CD86  
254 expression was significantly greater after treatment by ATCC25526 than UMB-MBP-01  
255 ( $P < 0.01$ ) (**Figure 2A-D**). Treatment with ATCC25526 cells stimulated increased MHC  
256 class II, while treatment with UMB-MBP-01 cells stimulated increased CD80 expression.  
257 Neither UMB-MBP-01 EPS nor ATCC25526 EPS altered expression of these surface  
258 receptors on BMDCs. For MΦ, ATCC25526 cells stimulated increased CD40, while

259 ATCC25526 EPS did not (**Figure 2E-G**). The other cell surface receptors were not  
260 affected by treatment with bacterial cells or EPS for M $\Phi$ . Overall, ATCC25526 and  
261 UMB-MBP-01 bacterial cells, but not EPS, triggered activation of important  
262 costimulatory receptors on innate myeloid cells *in vitro*, and these bacterial strains  
263 differed in these activities.

264 We next examined the effect of *Bifidobacterium* and EPS alone on cytokine  
265 production in innate immune cells. Both BMDC and M $\Phi$  showed increased secretion of  
266 IL-6, TNF $\alpha$ , and IL-10 when stimulated with UMB-MBP-01 and ATCC25526 strains.  
267 Induction of cytokine expression was also strain-specific as ATCC25526 cells  
268 stimulated a greater increase in IL-6 and IL-10 than UMB-MBP-01 cells in BMDCs  
269 (**Figure 3A, 3C**); and TNF $\alpha$  expression was also increased to a greater extent by  
270 ATCC25526 compared to UMB-MBP-01 with a borderline statistical significance ( $p =$   
271 0.059, **Figure 3B**). For M $\Phi$ , treatment with ATCC25526 cells increased TNF $\alpha$  compared  
272 to UMB-MBP-01 (**Figure 3E**), whereas there were no strain-specific differences in IL-6  
273 or IL-10 (**Figure 3D, 3F**). *B. pseudolongum* EPS did not stimulate cytokine production in  
274 either BMDC or M $\Phi$ . Similar to activation of co-stimulatory receptors, UMB-MBP-01 and  
275 ATCC25526 cells elicited unique myeloid cell cytokine responses that differed from one  
276 another and were not recapitulated by EPS.

277 *Bifidobacterium* strains induce distinct changes in local and systemic leukocyte  
278 distribution and lymph node morphology

279 We next assessed whether *Bifidobacterium* strains differentially induced changes  
280 in immune cell distribution and lymph node (LN) architecture *in vivo* using a mouse  
281 model. As illustrated in **Figure 4A**, mice received broad spectrum antibiotics for 6 days,

282 a regimen that depleted endogenous microbiota [44], followed by oral gavage with each  
283 bacterial strain or their EPS, and then daily immunosuppression with tacrolimus (3  
284 mg/kg/d s.c.). Two days after gavage, mesenteric and peripheral LNs (MLN and PLN)  
285 and intestinal tissues were harvested, and the intraluminal fecal content was collected  
286 for gut microbiome characterization. The effect of these microbiota on the distribution of  
287 immune cell populations was assessed by immunohistochemistry of intestinal segments  
288 and flow cytometry and immunohistochemistry of LNs.

289         Within the small intestine, both UMB-MBP-01 and ATCC25526 cells resulted in  
290 significantly more Foxp3+ regulatory T cells (Treg) compared to PBS control, while  
291 UMB-MBP-01 resulted in significantly more Treg compared to ATCC25526 (**Figure 4B**,  
292 flow cytometry gating protocol listed in **Supplemental Figure 3**). Gavage with UMB-  
293 MBP-01 EPS, but not ATCC25526 EPS, resulted in increased Treg compared to control  
294 (**Figure 4B**). ATCC25526 and UMB-MBP-01 cells resulted in more DC compared to  
295 PBS control, while ATCC25526 cells also resulted in more DC compared to UMB-MBP-  
296 01 cells (**Figure 4C**). UMB-MBP-01 and ATCC25526 EPS resulted in increased DC  
297 compared to PBS control, while UMB-MBP-01 EPS also resulted in more DC compared  
298 to ATCC25526 EPS (**Figure 4C**). Intestinal M $\Phi$  did not significantly change after whole  
299 bacteria or EPS gavage.

300         By flow cytometry, we observed decreased MLN Treg in UMB-MBP-01 EPS  
301 treated animals, but otherwise there were no other differences in the number and  
302 proportion of innate myeloid (DC, M $\Phi$ ) or adaptive lymphoid (CD4 T cells, CD8 T cells,  
303 Treg, and B cells) cells in the MLN or PLN of mice treated with the *B. pseudolongum*

304 strains compared to those treated with antibiotics alone or untreated controls  
305 **(Supplemental Figure 4A-L).**

306 For LN immunohistochemistry, we focused on the LN cortex because our  
307 previous work showed that architectural and cellular changes within this zone were  
308 most critical in mediating immune tolerance and suppression [45]. Within the MLN and  
309 PLN T cell cortex, neither gavage with whole bacteria nor EPS affected the number of  
310 Treg present, as measured by immunohistochemistry. This contrasts with the flow  
311 cytometry results above which showed that UMB-MBP-01 EPS caused a decrease in  
312 MLN Treg **(Supplemental Figure 4D)**. The difference between the flow cytometry and  
313 histologic results for Treg is likely due to the focus of histology analysis only on cells in  
314 the cortex while the flow cytometry summates all the cells in the entire LN. Gavage with  
315 whole bacteria and EPS from both strains increased DCs in the cortex of MLN  
316 compared to control **(Figure 4D)**, while the number of DC enumerated by flow  
317 cytometry did not change in MLN or PLN **(Supplemental Figure 4 E, K)**, with these  
318 differences again likely due to the factors noted above. M $\Phi$  increased in the cortex of  
319 MLN after whole bacteria or EPS treatments from both strains **(Figure 4E)**, but not in  
320 PLN **(Supplemental Figure 4N)**. ATCC25526 cells also resulted in a greater increase  
321 in MLN M $\Phi$  compared to UMB-MBP-01 cells **(Figure 4E)**. This result contrasts with flow  
322 cytometry data where there was no difference in M $\Phi$  populations in MLN or PLN after  
323 treatment.

324 Overall, gavage with whole bacteria and EPS altered gut associated innate  
325 myeloid cells and Tregs without affecting systemic distribution, as evidenced by  
326 unchanged PLN populations **(Supplemental Figure 4 M, N)**. Gavage with whole

327 *Bifidobacterium* cells led to increased intestinal Treg and DCs as well as increased MLN  
328 M $\Phi$  and DCs compared to controls. EPS also produced most of these effects apart from  
329 ATCC25526 EPS lack of effect on intestinal Treg compared to control. UMB-MBP-01  
330 cells led to increased intestinal Treg compared to ATCC25526 cells. In contrast,  
331 ATCC25526 cells led to increased DC in both intestine as well as increased cortical  
332 MLN M $\Phi$  compared to UMB-MBP-01 cells. UMB-MBP-01 EPS caused increased  
333 intestinal DC compared to ATCC25526 EPS. In contrast to the *in vitro* findings where  
334 EPS was generally inactive, *in vivo* treatment with EPS alone stimulated similar innate  
335 myeloid cell and Treg increases in gut and MLN compared to increases induced by live  
336 bacterial cells.

337         Since LN stromal fiber structures are important mediators of immune responses  
338 [46], we next assessed LN architecture using the ratio of laminin  $\alpha$ 4 to laminin  $\alpha$ 5 in the  
339 LN T cell cortex of the cortical ridge (CR) and around the high endothelial venules  
340 (HEV). An increased laminin  $\alpha$ 4: $\alpha$ 5 ratio is indicative of immune tolerance and  
341 suppression [45]. In the MLN CR, both UMB-MBP-01 and ATCC25526 increased the  
342 laminin  $\alpha$ 4: $\alpha$ 5 ratio, with UMB-MBP-01 cells causing a greater increase compared to  
343 ATCC25526 cells (**Figure 4F**). The laminin  $\alpha$ 4: $\alpha$ 5 ratio was not changed around the  
344 MLN HEV by either whole bacteria or EPS (**Supplemental Figure 4O**). In PLN CR, only  
345 UMB-MBP-01 cells resulted in an increased laminin  $\alpha$ 4: $\alpha$ 5 ratio (**Figure 4G**). Overall,  
346 gavage with both *B. pseudolongum* strains increased local MLN CR laminin  $\alpha$ 4: $\alpha$ 5  
347 ratios, while only UMB-MBP-01 increased the laminin  $\alpha$ 4: $\alpha$ 5 ratio in systemic PLN CR.  
348 This effect was more prominent for UMB-MBP-01 compared to ATCC25526,  
349 demonstrating strain-specific differences in immune modulation.

350 Markedly different intestinal transcriptional activities in response to UMB-MBP-01 than  
351 to ATCC25526

352 To determine the effect of UMB-MBP-01 and ATCC25526 on host gene  
353 expression, we characterized the transcriptome of mouse intestinal tissues harvested  
354 two days after gavage with either UMB-MBP-01, ATCC25526, or no bacteria control.  
355 Differentially expressed genes (DEGs) were identified by comparing the two treatment  
356 groups to the control and revealed both shared and strain-specific effects on  
357 transcription (**Supplemental Table 6B-D**). A total of 420 and 425 DEGs were observed  
358 in comparisons of UMB-MBP-01 vs. control and ATCC25526 vs. control, respectively,  
359 and 139 DEGs were observed comparing UMB-MBP-01 to ATCC25526 directly. Based  
360 on the log<sub>2</sub> fold change (LFC) scale of DEGs, the strongest intestinal response was  
361 elicited by UMB-MBP-01, compared to either ATCC25526 or control (**Supplemental**  
362 **Figure 5**). Functional enrichment analyses revealed the effects elicited by UMB-MBP-  
363 01 were mainly involved in positive regulation of cell activation, leukocyte and  
364 lymphocyte activation, B cell activation, and somatic recombination of immunoglobulin  
365 superfamily domains (**Supplemental Figure 5A, C**). Elicited effects of ATCC25526  
366 include responses in phagocytosis, membrane invagination, defense response to  
367 bacterium and complement activation (**Supplemental Figure 5E**). These results further  
368 supported our observations that ATCC25526 elicited distinct host responses compared  
369 to UMB-MBP-01, which induced greater numbers of DEGs and stronger host  
370 responses.

371 We further examined the host responses present in both UMB-MBP-01 and  
372 ATCC25526 as well as those present only in one but not the other, to pinpoint the

373 differential host responses induced by the two strains. Of the DEGs identified comparing  
374 UMB-MBP-01 or ATCC25526 to the control (n=411 and 416), 59.6% and 58.9%,  
375 respectively, were identified in both comparisons (**Figure 2A, Supplemental Table 6**).  
376 These overlapped DEGs (N=238) and the condition-specific DEGs, that included 164  
377 DEGs only up-regulated in UMB-MBP-01 versus control and 111 DEGs only  
378 upregulated in UMB-MBP-01 versus ATCC25526, comprised the majority of all DEGs  
379 (85.9%). Downregulated genes accounted for only a small fraction of all DEGs (14.1%)  
380 and majority of them were identified in only the comparison of UMB-MBP-01 vs.  
381 ATCC25526 (N=67, 80.1% of downregulated). The DEGs that were upregulated in both  
382 UMB-MBP-01 vs. control and ATCC25526 vs. control include B cell immunity, collagen  
383 metabolism, immunoglobulin protein expression, cytokines (IL-1 $\beta$ , IL-10, IL-13, IL-21),  
384 TNF receptor superfamily, among others (**Supplemental Table 6**). Two functional  
385 pathways were enriched in UMB-MBP-01 vs control, but not in ATCC25526 vs control:  
386 regulation of cell-cell adhesion and T cell activation and the response to interferon  $\gamma$  and  
387 interferon  $\beta$  (**Figure 5B**). In contrast, the host responses to ATCC25526 but not UMB-  
388 MBP-01 were enriched in functions involved in fatty acid metabolism, lipid localization,  
389 acylglycerol metabolism, and cholesterol and sterol homeostasis (**Supplemental**  
390 **Figure 5D**). Together these data further indicated that the effects of UMB-MBP-01 or  
391 ATCC25526 were mediated through different pathways. The ATCC25526 strain  
392 appeared to exert immunomodulatory effects, at least in part, via stimulation of  
393 phagocytosis and induced lipid metabolism, while the UMB-MBP-01 strain exerted  
394 stronger effects, mostly through upregulating antibody secretion and regulation of  
395 multiple aspects of lymphocyte functions, including cytokines, adhesion, and activation.

396 As extracellular molecules may play an important role in eliciting  
397 immunomodulatory effects, we also compared intestinal gene expression following  
398 gavage with live *B. pseudolongum* bacteria to that with *B. pseudolongum* produced  
399 EPS. The comparison revealed DEGs that were mostly group-specific without much  
400 overlap with EPS vs. control group (12.1%, N=39) (**Supplemental Figure 6A, B**).  
401 These data indicated that the predominant intestinal transcriptional responses were due  
402 to *B. pseudolongum* whole cell gavage (62.6%, N=201), compared to DEGs in EPS  
403 gavage (25.5%, N=82). Gene-pathway network analyses indicated B cell receptor  
404 activation and signaling, antigen-receptor mediated signaling, and phagocytosis  
405 recognition and engulfment were highly upregulated by whole *B. pseudolongum* gavage  
406 (**Supplemental Figure 6C**). While both live cells and EPS induced antimicrobial  
407 circulating immunoglobulin, the transcriptional effects were an order of magnitude  
408 higher for live cells (**Supplemental Figure 6C-D**). This result was commensurate with  
409 the observations above that EPS did not stimulate cytokine production or cell surface  
410 costimulatory receptor expression in either BMDC or M $\Phi$ . Together, our data suggested  
411 that the immunomodulatory effects of *B. pseudolongum* were potentially via their  
412 metabolic activities and secreted molecules and/or other cell membrane components  
413 other than the surface structure of EPS.

414 Different *B. pseudolongum* strains elicit rapid, profound alterations in both structure and  
415 function of gut microbiome

416 We next investigated the impact of bacterial gavage on the gut microbiome using  
417 shotgun metagenomic sequencing of the intraluminal fecal content (40.6 $\pm$ 7.7 million  
418 reads per sample; **Supplemental Table 2B**). Taxonomic composition was established

419 using the comprehensive mouse gut metagenome catalog (CMGM) [47] designed  
420 specifically to characterize the mouse gut microbiome (**Figure 5A, Supplemental Table**  
421 **7**). A significant reduction in gut microbial community diversity was observed after both  
422 UMB-MBP-01 and ATCC25526 gavage, with UMB-MBP-01 gavage resulting in the  
423 lowest diversity (**Figure 5C**). After *B. pseudolongum* administration, the most  
424 outstanding changes in specific taxonomic groups were the marked increases in the  
425 relative abundance of *Bacteroides thetaiotaomicron* and *Lactobacillus johnsonii* and  
426 relative depletion of *Muribaculaceae* and *Erysipelotrichaceae* (**Figure 5B,**  
427 **Supplemental Figure 7**). Gavage with the *Desulfovibrio* did not produce a significant  
428 change in the microbiome, and *Muribaculaceae*, *Erysipelotrichaceae*, and  
429 *Lachnospiraceae* were the most abundant groups in these communities and in the not-  
430 treatment control communities. These data indicated the gavage of either *B.*  
431 *pseudolongum* strains profoundly altered the gut microbial community, with a significant  
432 reduction in abundance of endogenous gut microorganisms.

433 Canonical Correspondence Analysis (CCA) on both community taxonomic  
434 profiles and functional pathways resulted in concordant clustering patterns, in that  
435 ATCC25526 or UMB-MBP-01 each resulted in a distinct community, and that were  
436 clearly separate from *Desulfovibrio*-treated and no bacteria controls (**Figure 5D, 5E**).  
437 Based on linear discriminant analysis (LDA) effect size (LEfSe) analysis [48], UMB-  
438 MBP-01 resulted in a significantly higher abundance of *B. pseudolongum* than  
439 ATCC25526 (19.8±6.1% vs. 6.1%±2.0%, P = 0.02, **Supplemental Figure 8A,B**). These  
440 data suggested murine strain UMB-MBP-01 was better able to colonize the mouse gut  
441 than the porcine isolate ATCC25526, lead to greater abundance in the murine gut

442 environment. On the other hand, *Enterobacteriaceae* (*Klebsiella michiganensis* and  
443 *Enterobacter himalayensis*), and *Clostridiaceae* (*Clostridium paraputrificum* and  
444 *Clostridium* MGG49300) were significantly more enriched in the ATCC25526 treated  
445 group but were mostly absent in the UMB-MBP-01 gavage mice (**Supplemental Figure**  
446 **8C-F**). Based the scaled eigenvalue, the top taxa and pathways that contributed to the  
447 separation of the clusters in ordination analyses were identified (**Supplemental Figure**  
448 **9A, B, Supplemental Table 8**). The ATCC25526 cluster was attributed to  
449 *Enterobacteriaceae* and *Clostridiaceae*, and the top contributors included *K.*  
450 *pneumonia*, *K. michiganensis*, *B. animalis*, *E. himalayensis*, and *Clostridium*  
451 *paraputrificum*. The most prominent pathways attributed to ATCC25526 cluster include  
452 motility (peptidoglycan maturation), gluconeogenesis, energy conversion (fatty acid  $\beta$ -  
453 oxidation), and L-threonine biosynthesis. On the other hand, *Akkermansia muciniphila*,  
454 *Paeniclostridium sordellii*, and *B. pseudolongum* were among the top significant  
455 contributors to the UMB-MBP-01 cluster. The most outstanding pathways for UMB-  
456 MBP-01 included ribonucleotide and amino acid biosynthesis (folate transformation, L-  
457 isoleucine, L-arginine, L-lysine) and pyruvate fermentation (pyruvate/acetyl-CoA  
458 pathway). Together, the data indicated UMB-MBP-01 or ATCC25526 each altered the  
459 gut microbiota profoundly and distinctively, which may contribute to their distinct  
460 immunomodulatory effect.

## 461 Discussion

462 *B. pseudolongum* demonstrates great intraspecies genetic diversity and shows  
463 patterns consistent with host specificity, rendering it an advantageous model organism  
464 to study the effect of intraspecies variation on host immunomodulation [35]. Further, as  
465 a predominant species in the murine GI tract, *B. pseudolongum* displays an extensive  
466 enzymatic capacity and might act as a keystone species in this environment [35, 49]. In  
467 this study, we employed the murine strain UMB-MBP-01, which demonstrates an anti-  
468 inflammatory and pro-homeostatic effect [33, 34], and porcine-isolated *B.*  
469 *pseudolongum* type strain ATCC25526 to investigate the strain-specific mechanisms of  
470 host responses *in vitro* and *in vivo*. The distinct genetic attributes and  
471 immunomodulatory capabilities of UMB-MBP-01 from the *B. pseudolongum* type strain  
472 ATCC25526 show that *Bifidobacterium* modulates intestinal responses and host  
473 immunity in a strain specific manner. We observed UMB-MBP-01 exerted stronger  
474 immunologic effects in intestinal responses mostly likely through regulation of multiple  
475 aspects of lymphocyte functions, while ATCC25526 appeared to exert  
476 immunomodulatory effects, at least in part, via stimulation of phagocytosis and induced  
477 lipid metabolism. We further demonstrated the *in vitro* strain-specific activation and  
478 cytokine responses in DC and M $\Phi$  and changes in local and systemic leukocyte  
479 distribution and LN morphology, demonstrating the unique immune modulatory effects  
480 of the two *B. pseudolongum* strains. A deeper understanding of strain-specific  
481 immunomodulatory properties is fundamentally important to inform probiotic design as  
482 well as immunomodulatory therapeutic targeting.

483           It remains unclear whether *B. pseudolongum* immune and intestinal modulation  
484 is mediated through direct interactions with the intestinal epithelium, or indirectly via  
485 modulation of endogenous gut microbiome with consequent effects on intestinal  
486 metabolism and immunity, or both [18]. In our study, the administration of two separate  
487 *B. pseudolongum* strains resulted in profoundly different gut microbiomes in both  
488 structure and functional capabilities as well as intestinal responses, suggesting the  
489 critical involvement of the endogenous gut microbiome as a key element of their  
490 immunomodulatory attributes and indicating that indirect effects likely contribute. Our  
491 results align with recent key clinical findings, suggesting that *Bifidobacterium* could act  
492 as a “microbiome modulator” to competitively exclude toxigenic pathogens and  
493 orchestrate homeostatic gut metabolism and host immune responses [50-53]. It is worth  
494 noting that the effect of LBPs on the structure and function of the microbial community  
495 has not been accepted among standard parameters to characterize or evaluate LBP  
496 efficacy. Our study emphasizes the importance of characterization of the dynamics of  
497 the gut microbial community to understand the efficacy and specificity of LBPs.

498           Distinctive from ATCC25526 and pro-inflammatory bacterial control, UMB-MBP-  
499 01 demonstrated strain persistence within the gut microbiome after administration,  
500 further highlighting the role of gut microbiome in LBP-host interaction. Previous studies  
501 suggested that the administration of *B. longum* subsp. *longum* has stable, persistent  
502 colonization in recipients whose gut microbiome previously had low abundance of gene  
503 content involved in carbohydrate utilization, suggesting competition for resources as a  
504 key mechanism determining strain persistence [54]. This may relate to the ecological  
505 concept of “colonization resistance”, whereby endogenous microbiota occupy host

506 tissues with an intrinsic capability to limit the introduction of exogenous microorganisms  
507 and the expansion of endogenous microorganisms, while a microbiota with low capacity  
508 in carbohydrate assimilation could be more permissive to exogenous colonization that  
509 can fundamentally disrupt the microbiota [55, 56]. Given human gut reliance on  
510 microbiota to cope with glycan-rich gut environment for the metabolism of luminal  
511 oligosaccharides [57], the ability of *Bifidobacterium* strains to utilize complex  
512 carbohydrates provides a selective advantage to effectively compete for nutrients with  
513 other bacteria in the gut microenvironment [57]. Interestingly, their repertoire of  
514 glycoside hydrolases are species- or strain-specific [39, 58], indicating indispensable  
515 roles for glycan-assimilation in their specific niche adaptability to the intestinal  
516 microenvironment. Supporting the competitive exclusion ecological theory, we observed  
517 the depletion of endogenous gut microorganisms *Muribaculaceae* and  
518 *Erysipelotrichaceae* with *Bifidobacterium* treatment, as well as the specialized  
519 carbohydrate metabolism of UMB-MBP-01 in utilizing a greater variety of  
520 oligosaccharide molecules and host-derived glycans. Future longitudinal  
521 characterization of strain persistence, microbiota changes, and oligosaccharide and  
522 glycoprotein assimilation may hold a key to determine probiotic strain specificity in host  
523 adaption and intestinal responses.

524         The bacterial determinants of immunomodulation properties of individual strains  
525 remains an underdeveloped research area. Recent studies revealed strains of the same  
526 species induced different immunophenotypes, suggesting that bacterial-induced  
527 immunomodulation is not dictated by bacterial phylogeny [22, 59]. Multiple LBP  
528 produced effector molecules that interact with host immunity have been recently

529 identified [60]. In particular, cell wall components found in Gram-positive bacteria, such  
530 as peptidoglycan and lipoteichoic acid, contain MAMPs which are recognized by  
531 immunoregulatory pattern recognition receptors such as Toll-like receptors [23].  
532 *Bifidobacterium* peptidoglycans have also demonstrated immunomodulatory effects on  
533 the Th1 polarization of naïve T cells as well as DC maturation and enhanced immune  
534 responses [61, 62]. Other surface molecules such as EPS and pili also play a role in  
535 *Bifidobacterium*'s strain-specific pro-homeostatic immunomodulation [27, 28]. We also  
536 observed here expanded enzymatic capabilities of UMB-MBP-01, but not ATCC25526,  
537 in assimilating oligosaccharide molecules and host-derived glycans as well as the  
538 capacity to manufacture cell wall components such as peptidoglycan. Together these  
539 studies implicate the genetic variation of different bacterial strains as underlying induced  
540 intestinal responses and mucosal immunological signaling. This speculation warrants  
541 direct experimental validation.

542         Making conclusions about the immunomodulatory effects of bacterial strains  
543 based on the surface structures alone is inaccurate, as the preparations of the cell wall  
544 components and extracellular polysaccharides are strongly influenced by cultivation  
545 conditions [63]. The differences observed in this study between *Bifidobacterium* whole  
546 cells and purified EPS *in vitro* vs. *in vivo* indeed suggest the presence of many other  
547 molecules and mechanisms that contribute to the regulation of immunity and  
548 inflammation. In particular, the observation that EPS alone yielded gut Treg recruitment  
549 in addition to innate myeloid cell populations suggests that EPS may act indirectly  
550 through an intermediary, such as intestinal epithelial cells, which then influence  
551 leukocyte subsets. Indeed, characterization of *B. pseudolongum*-induced innate

552 immune responses revealed that these bacteria induce a more balanced anti-  
553 inflammatory and homeostatic cytokine response from DC and M $\Phi$  [64]. In addition, *B.*  
554 *pseudolongum* induced changes in LN architecture, resulting in an increased ratio of  
555 extracellular matrix protein laminin  $\alpha$ 4 to laminin  $\alpha$ 5 in the cortical ridge, a microdomain  
556 structure that is mechanistically associated with immunologic suppression and tolerance  
557 [33]. These observations demonstrate that a single probiotic bacterial strain can  
558 influence local, regional, and systemic immunity through both innate and adaptive  
559 pathways. A holistic understanding of the strain-specific bacterial effects is critical to  
560 inform probiotic design as well as immunomodulatory therapeutic targeting.

561 **Conclusion**

562           The distinct genetic attributes and immunomodulatory capabilities of UMB-MBP-  
563 01 compared to *B. pseudolongum* type strain ATCC25526 show that *Bifidobacterium*  
564 modulates intestinal responses and host immunity in a strain-specific manner. Our  
565 results highlight the importance to characterize individual *Bifidobacterium* strains and  
566 not to generalize their immunomodulatory effects to other strains of the same species,  
567 despite their many shared features. It is critical to investigate both endogenous  
568 microbiota in response to LBP strains and to profile the intestinal responses, in order to  
569 interrogate mechanistically the highly coordinated multicellular host-microbe  
570 interactions, which are key to understanding strain-specific immunomodulation. Future  
571 studies are warranted to investigate the specific bioactive metabolites and pathways  
572 through which the gut microbiota exert their immunomodulatory effects, and the specific  
573 intestinal cell types that respond to those signals. A comprehensive understanding of  
574 strain-specific immunomodulatory properties is fundamentally important to inform  
575 probiotic design as well as immunomodulatory therapeutic targeting.

576 **Methods and Materials**

577 Strains cultivation and genomic sequencing

578 *B. pseudolongum* strain ATCC25526 was purchased from ATCC (Manassas, Virginia).

579 *B. pseudolongum* strain UMB-MBP-01 was isolated from the feces of C57BL/6J mice

580 through passages and screening on Bifidus Selective Medium (BSM) agar (Sigma-

581 Aldrich, St. Louis, MO, USA), as previously described [34]. Both strains were initially

582 grown anaerobically at 37°C for 3–5 days on Bifido Selective Media (BSM) agar plates

583 (Millipore Sigma, Burlington, MA), from which a single colony was selected and grown in

584 BSM broth (Millipore Sigma, 90273-500G-F) until stationary phase (up to 3 days).

585 *Desulfovibrio desulfuricans subsp. desulfuricans* (ATCC27774) was purchased from

586 ATCC and grown in ATCC Medium: 1249 Modified Baar's Medium (MBM) for sulfate

587 reducers, which was made according to ATCC protocol. Cultures were initially

588 incubated under anaerobic conditions for 5 days on Modified Baar's Medium agar

589 plates, after which single colonies were chosen, transferred to liquid media, and

590 incubated for up to 3 weeks. *B. pseudolongum* strains ATCC25526 and UMB-MBP-01

591 were used in cell stimulation and cytokine assays.

592 *B. pseudolongum* UMB-MBP-01 was sequenced previously [34]. For strain

593 ATCC25526, genomic DNA extraction was performed using a lysozyme/mutanolysin-

594 based cell lysis followed by purification using the Wizard Genomic DNA Purification Kit

595 (Promega, Madison, WI, USA). Library preparation on extracted DNA was conducted

596 using a Kapa kit (Roche, Indianapolis, IN) for 150-bp paired-end sequencing, and

597 sequencing was performed with an Illumina (San Diego, CA) MiSeq system.

598 Sequencing was performed by the University of Maryland School of Medicine, Institute

599 for Genome Sciences, Genomics Resource Center with standard operating procedures  
600 and assembled using SPAdes v3.14.0 [65]. Contig ordering was performed using  
601 MAUVE contig mover [66] and the UMB-MBP-01 genome as reference [67].

#### 602 Exopolysaccharide (EPS) Isolation

603 EPS was extracted from strains X and Y using the protocol previously published  
604 by Bajpai and colleagues [68]. Briefly, bacterial cultures were grown in 500 ml BSM  
605 media to early stationary phase, after which trichloroacetic acid was added (14% v/v  
606 final) and the mixture incubated at 37°C for 40 minutes. After centrifugation at 8,000 g  
607 for 20 minutes at 4°C, the supernatant was collected, absolute ethanol added (2:1 v/v  
608 EtOH:sup), followed by incubation at 4°C for 48h and centrifugation at 8,000xg at 4°C  
609 for 20 minutes. This ethanol wash step was repeated to remove any impurities, and a  
610 final centrifugation at 8,000xg at 4°C for 20 minutes was performed. The resulting pellet  
611 was then dissolved in 5 to 10 ml of water, before being dialyzed against DI water for 48  
612 hours, and lyophilized.

#### 613 Anaerobic microplate assay

614 Anaerobic microplates (AN plates, Biolog, Hayward, CA) pre-coated with 95  
615 various carbon sources was used in the assay. Each well of the 96-well AN Biolog plate  
616 was coated by a sole-carbon source, with one well being used as no carbon control.  
617 Metabolism of the substrate in particular wells results in formazan production, producing  
618 a color change in the tetrazolium dye. Cultured bacteria in log growth phase were  
619 centrifuged down to pellet, which was suspended using inoculating fluid (Biolog,  
620 Hayward, CA) to an OD value around 0.26. The suspension was added to the

621 microplates and sealed by anaerobic GasPak EZ anaerobe gas pouch system with  
622 anaerobic indicators (BD, Franklin Lakes, NJ). The plates were read between 20-24hrs  
623 following inoculation with a pre-grown isolate using spectrophotometer microplate  
624 reader (Molecular Devices, LLC, San Jose, CA) and reading data acquisition was  
625 performed using SoftMax Pro 7 software (Molecular Devices, LLC, San Jose, CA). The  
626 procedure was performed in triplicate for each strain. The no carbon control reading  
627 was subtracted from each of the readings of the wells, and student's t test was  
628 performed to test if the average reading was significantly different from zero.

### 629 Comparative genomics analyses

630       A total of 79 *B. pseudolongum* genomes were included in the analyses, which  
631 included the four sequenced in this study and all 75 available *B. pseudolongum*  
632 genomes on GenBank (retrieved September 2021, **Supplemental Table 5A**). The  
633 pangenome was constructed using anvio vers 6.2 workflow [69, 70]. Briefly, this  
634 workflow 1) dereplicates genomes based on similarity score calculated using Sourmash  
635 vers 3.3 [71], 2) uses BLASTP to compute ANI identity between all pairs of genes, 3)  
636 uses the Markov Cluster Algorithm (MCL) [72] to generate homologous gene clusters  
637 (HGCs) based on all-versus-all sequence similarity, and 4) aligns amino acid sequences  
638 using MUSCLE [73] for each gene cluster. Each gene was assigned to core or  
639 accessory according to the hierarchical clustering of the gene clusters. Sourmash vers  
640 3.3 [71] was used to compute ANI across genomes. Functional annotation of each  
641 secreted protein was performed employing the eggNOG database v5.0 [74] using  
642 eggNOG-mapper v2 [75] and the results were imported into the anvio contig database.  
643 Further functional annotation included PFAMs based on hidden Markov model (HMM)

644 search to Pfam vers34.0 [76]. Protein-coding genes were also annotated to metabolic  
645 functionality categories using KEGG (Kyoto Encyclopedia of Genes and Genomes) [77].  
646 GhostKOALA annotation tool [78] was used to assign KEGG Identifiers. Enrichment  
647 analyses were performed using Anvi'o pangenome pipeline that take COG functions  
648 across genomes and clade affiliation as the explanatory variable. The equality of  
649 proportions across clade affiliation was tested using a Rao score test, which generates  
650 an enrichment score as the test statistic and a p value. The q-value was then calculated  
651 from the p value to account for multiple testing using R package qvalue [79]. A COG  
652 function was considered enriched if the q-value was below 0.05.

653         The prediction of genes encoding extracellular enzymes possessing structurally  
654 related catalytic and carbohydrate-binding modules catalyzing hydrolysis, modification,  
655 or synthesis of glycoside bounds was performed using dbCAN2 [80] and dbCAN  
656 HMMdb (v.9) that was built using CAZy database (v.07302020) [38]. To identify signal-  
657 peptide specific sequence motifs, we employed the subcellular localization prediction  
658 tool PSORTb (v.3.0.2) [81].

### 659 *In vitro* co-culture

660 Peritoneal macrophages (M $\Phi$ ) and bone marrow derived dendritic cells (BMDCs) were  
661 isolated and then seeded onto 24 well plates in 1 ml RPMI complete medium as  
662 described [82]. Briefly, M $\Phi$  were collected 4 days after i.p. injection of Remel  
663 Thioglycollate solution (Thermo Fisher Scientific, Waltham, MA). BMDCs were  
664 generated from bone marrow cells treated with 10 ng/ml GM-CSF (R&D Systems,  
665 Minneapolis, MN) for 10 days. Loosely adherent immature BMDCs were collected and  
666 then CD11c+ DCs were enriched using CD11c positive selection kit (Stemcell

667 Technologies, Cambridge, MA). Twenty-four hours after culture of purified subsets, the  
668 cells were stimulated with UV-killed *Bifidobacterium* bacteria or purified EPS for 24  
669 hours. Bacterial cells were killed by UV exposure at 100  $\mu\text{J}/\text{cm}^2$  for four 15-minute  
670 cycles with a UV CrossLinker (Fisher Scientific, Hampton, NH). Culture supernatants  
671 were collected from whole bacteria or EPS stimulated cultures and ELISA for TNF $\alpha$ , IL-  
672 6, and IL-10 (BioLegend, San Diego, CA) performed. The myeloid cells from co-culture  
673 wells were collected and analyzed by flow cytometry.

#### 674 Flow cytometry

675 Cells were passed through 70- $\mu\text{m}$  nylon mesh screens (Thermo Fisher Scientific,  
676 Waltham, MA) to produce single-cell suspensions. Cell suspensions were treated with  
677 anti-CD16/32 (clone 93, eBioscience) to block Fc receptors, and then stained for 30  
678 minutes at 4°C with antibodies against surface molecules (**Supplementary Table 9**)  
679 and washed 2 times in FACS buffer [phosphate buffered saline (PBS) with 0.5% w/v  
680 Bovine serum albumin (BSA)]. Samples were analyzed with an LSR Fortessa Cell  
681 Analyzer (BD Biosciences), and data analyzed with FlowJo software version 10.6 (BD  
682 Biosciences).

#### 683 Immunohistochemistry

684 Peripheral LN, mesenteric LN, and small bowel segment (duodenal-jejunal junction)  
685 were excised and washed in cold PBS before freezing in OCT (Sakura Finetek,  
686 Torrance, CA) in histology blocks on dry ice and then stored at -80°C. LN cryosections  
687 were cut in triplicate at 5  $\mu\text{m}$  using a Microm HM 550 cryostat (Thermo Fisher Scientific,  
688 Waltham, MA). Sections attached to slides were fixed with cold acetone/ethanol (1:1)

689 solution and washed in PBS buffer (Lonza, Morristown, NJ). Primary antibodies and  
690 isotype controls (**Supplementary Table 9**) were added to slides for 1 hour in a  
691 humidified chamber. Sections were washed with PBS, blocked with 2.5% donkey serum  
692 and 2.5% goat serum, and incubated with secondary antibodies for 60 minutes. Slides  
693 were then fixed with 4% paraformaldehyde/PBS (Alfa Aesar, Haverhill, MA) for 5  
694 minutes, incubated with 1% glycerol for 5 minutes, and Prolong Gold Antifade Mountant  
695 with or without DAPI (Thermo Fisher Scientific, Waltham, MA) was added before  
696 applying cover slips. Images were acquired using an Accu-Scope EXC-500 fluorescent  
697 microscope (Nikon, Melville, NY) and analyzed with Volocity image analysis software  
698 (PerkinElmer, Waltham, MA). The percentage positive staining area was quantified  
699 based on at least 2 independent experiments with 3 mice/group, 3 LNs/mouse, 3  
700 sections/LN, and 3–5 fields/section.

#### 701 Mice experiments

702 Female C57BL/6 mice between 8 and 14 weeks of age were purchased from The  
703 Jackson Laboratory (Bar Harbor, ME). All the procedures involving mice were performed in  
704 accordance with the guidelines and regulations set by the Office of Animal Welfare  
705 Assurance of the University of Maryland School of Medicine, under the approved  
706 IACUC protocols 0518004 and 0121001. Mice were fed antibiotics (kanamycin,  
707 gentamicin, colistin, metronidazole, and vancomycin) *ad libitum* in drinking water on  
708 days -6 to -1. On day 0, cultured *Bifidobacterium* ATCC25526 or UMB-MBP-01 were  
709 gavaged p.o. Mice received tacrolimus (3 mg/kg/d s.c.) on days 0 and 1. On day 2, the  
710 animals were euthanized. Mesenteric and peripheral (axillary, inguinal, popliteal,  
711 brachial) LNs as well as small intestine were harvested. Fecal pellets were also

712 collected prior to euthanasia into individual tubes, using aseptic technique to minimize  
713 handling, and stored at -80°C. Antibiotics were USP grade or pharmaceutical secondary  
714 standard (all from MilliporeSigma): kanamycin sulfate (0.4 mg/ml), gentamicin sulfate  
715 (0.035 mg/ml), colistin sulfate (850 U/ml), metronidazole (0.215 mg/ml), and  
716 vancomycin hydrochloride (0.045 mg/ml) were dissolved in vivarium drinking water and  
717 administered *ad libitum*. Tacrolimus (USP grade, MilliporeSigma) was reconstituted in  
718 DMSO (USP grade, MilliporeSigma) at 20 mg/ml and diluted with absolute ethanol (USP  
719 grade, Decon Labs, King of Prussia, PA) to 1.5mg/ml. DMSO/ethanol stock was diluted  
720 1:5 in sterile PBS for s.c. injection and injected at 10 µl/g (3 mg/kg/day).

#### 721 Metagenomic sequencing and microbiome analyses

722 Harvested intestine tissues and luminal contents were stored immediately in  
723 DNA/RNA Shields (Zymo Research, Irvine, CA) to stabilize and protect the integrity of  
724 nucleic acids and minimize the need to immediately process or freeze specimens. The  
725 colon content from ~1cm colon tissue was used in DNA extraction. Metagenomic  
726 sequencing libraries were constructed from the same DNA using the Nextera XT Flex kit  
727 (Illumina) according to the manufacturer recommendations. Libraries were then pooled  
728 together in equimolar proportions and sequenced on a single Illumina NovaSeq 6000  
729 S2 flow cell at the Genomic Resource Center of the Institute for Genome Sciences at  
730 the University of Maryland School of Medicine.

731 Metagenomic sequence reads were removed using BMTagger v3.101 [83] using  
732 a Genome Reference Consortium Mouse Build 39 of strain C57BL/6J (GRCm39) [84].  
733 Sequence read pairs were removed even if only one of the reads matched to the mice  
734 genome reference. The Illumina adapter was trimmed and quality assessment was

735 performed using default parameters in fastp (v.0.21.0) [85]. The taxonomic composition  
736 of the microbiomes was established using Kraken2 (v.2020.12) [86] and Braken (v.  
737 2.5.0) [87] using the comprehensive mouse gut metagenome catalog (CMGM) [47] to  
738 calculate the metagenomic taxonomic composition. The Phyloseq (v.1.34.0) [88] R  
739 package was used to generate the diversity plot and barplot. Linear discriminant  
740 analysis (LDA) effect size (LEfSe) analysis [48] was used to identify fecal phylotypes  
741 that could explain differences between. For LEfSe, only taxonomic groups present  
742 in >1% of at least one sample were included in the analyses; the alpha value for the  
743 non-parametric factorial Kruskal-Wallis (KW) sum-rank test was set at 0.05 and the  
744 threshold for the logarithmic LDA model [89] score for discriminative features was set at  
745 2.0. An all-against-all BLAST search in multi-class analysis was performed.  
746 Metagenomics dataset was mapped to the protein database UniRef90 [90] to ensure  
747 the comprehensiveness in functional annotation, and was then summarized using  
748 HUMAnN2 (Human Microbiome Project Unified Metabolic Analysis Network) (v0.11.2)  
749 [91] to efficiently and accurately determine the presence, absence, and abundance of  
750 metabolic pathways in a microbial community. Further, HUMAnN2 employed a tiered  
751 search strategy enabling a species-resolved functional profiling of metagenomes, hence  
752 to characterize the contribution to the functional pathways of a known species.  
753 Canonical Correspondence Analysis (CCA) was used in ordination analysis, and biplot  
754 was generated using vegan package [92, 93] based on bray-curtis distance. CA1 and  
755 CA2 were selected as the major components based on the eigenvalue. A species score  
756 was scaled proportional to the eigenvalues representing the direction from the origin  
757 where the group had a larger than average value for the particular species [92, 94]. The

758 species scores greater than 1 were used to select the species that were considered the  
759 most significant contributors to each group.

#### 760 RNA isolation, transcriptome sequencing and analyses of the intestinal tissues

761 Dissected intestinal tissues were stored immediately in RNAlater solution  
762 (QIGEN) that had been stored at  $-80^{\circ}\text{C}$  to stabilize and protect the integrity of RNA  
763 [95]. For each sample, bulk RNA was extracted from  $\sim 1\text{cm}$  of intestine tissues. Prior to  
764 the extraction,  $500\mu\text{l}$  of ice-cold RNase free PBS was added to the sample. To remove  
765 the RNAlater, the mixture was centrifuged at  $8,000\times g$  for 10min and the resulting pellet  
766 resuspended in  $500\mu\text{l}$  ice-cold RNase-free PBS with  $10\mu\text{l}$  of  $\beta$ -mercaptoethanol. Tissue  
767 suspension was obtained by bead beating procedure using the FastPrep lysing matrix B  
768 protocol (MP Biomedicals, Solon, OH) to homogenized tissues. RNA was extracted  
769 from the resulting suspension using TRIzol Reagent (Invitrogen, Carlsbad, CA) following  
770 the manufacturer recommendations and followed by protein cleanup using Phasemaker  
771 tubes (Invitrogen) and precipitation of total nucleic acids using isopropanol. RNA was  
772 resuspended in DEPC-treated DNAase/RNAase-free water. Residual DNA was purged  
773 from total RNA extract by treating once with TURBO DNase (Ambion, Austin, TX, Cat.  
774 No. AM1907) according to the manufacturer's protocol. DNA removal was confirmed via  
775 PCR assay using 16S rRNA primer 27F (5'-AGAGTTTGATCCTGGCTCAG-3') and  
776 534R (5'-CATTACCGCGGCTGCTGG-3'). The quality of extracted RNA was verified  
777 using the Agilent 2100 Expert Bioanalyzer using the RNA 1000 Nano kit (Agilent  
778 Technologies, Santa Clara, CA). Ribosomal RNA depletion and library construction  
779 were performed using the RiboZero Plus kit and TruSeq stranded mRNA library  
780 preparation kit (Illumina) according to the manufacturer's recommendations. Libraries

781 were then pooled together in equimolar proportions and sequenced on a single Illumina  
782 NovaSeq 6000 S2 flow cell at the Genomic Resource Center (Institute for Genome  
783 Sciences, University of Maryland School of Medicine) using the 150 bp paired-end  
784 protocol.

785         Bioinformatic analysis of the transcriptome data includes the quality of fastq files,  
786 which was evaluated by FastQC. Reads were aligned to the mouse genome (v.  
787 *Mus\_musculus.GRCm39*) using HiSat (v. HISAT2-2.1.0) [96] and the number of reads  
788 that aligned to the coding regions were determined using HTSeq (v.1.0.0) [97].  
789 Significant differential expression was assessed using DEseq with an FDR value  $\leq 0.05$   
790 [98]. Quadrant plot to show whether DEGs have the same or opposite relationships  
791 between each of the pairwise comparisons of UMB-MBP-01 vs ATCC25526 and UMB-  
792 MBP-01 vs control. Gene Ontology (GO) enrichment analysis was performed in order to  
793 identify GO terms significantly over-represented in genes deregulated in specific  
794 comparisons and, as a result, to suggest possible functional characteristics of these  
795 genes. Enriched GO terms in the set of genes that are significantly over-expressed or  
796 under-expressed in a specific condition may suggest possible mechanisms of regulation  
797 or functional pathways that are, respectively, activated or repressed in that condition.  
798 Over-representation analyses [99] of differentially expressed genes (DEGs) against GO  
799 ontologies was performed using enrichGO function of clusterProfile Bioconductor  
800 package [100]. Cnetplot function was used to depict the linkages of genes and GO  
801 terms as a Gene-Concept Network for top over-represented GO terms based on q-value  
802 and gene-count.

803 **References**

- 804 1. Milani C, Turroni F, Duranti S, Lugli GA, Mancabelli L, Ferrario C, van Sinderen D, Ventura  
805 M: **Genomics of the Genus Bifidobacterium Reveals Species-Specific Adaptation to the**  
806 **Glycan-Rich Gut Environment.** *Appl Environ Microbiol* 2016, **82**:980-991.
- 807 2. O'Callaghan A, van Sinderen D: **Bifidobacteria and Their Role as Members of the**  
808 **Human Gut Microbiota.** *Front Microbiol* 2016, **7**:925.
- 809 3. Gionchetti P, Rizzello F, Venturi A, Campieri M: **Probiotics in infective diarrhoea and**  
810 **inflammatory bowel diseases.** *J Gastroenterol Hepatol* 2000, **15**:489-493.
- 811 4. Marteau P, Seksik P, Jian R: **Probiotics and intestinal health effects: a clinical**  
812 **perspective.** *Br J Nutr* 2002, **88 Suppl 1**:S51-57.
- 813 5. Sanders ME, Merenstein DJ, Reid G, Gibson GR, Rastall RA: **Probiotics and prebiotics in**  
814 **intestinal health and disease: from biology to the clinic.** *Nat Rev Gastroenterol Hepatol*  
815 2019, **16**:605-616.
- 816 6. Venturi A, Gionchetti P, Rizzello F, Johansson R, Zucconi E, Brigidi P, Matteuzzi D,  
817 Campieri M: **Impact on the composition of the faecal flora by a new probiotic**  
818 **preparation: preliminary data on maintenance treatment of patients with ulcerative**  
819 **colitis.** *Aliment Pharmacol Ther* 1999, **13**:1103-1108.
- 820 7. Patole SK, Rao SC, Keil AD, Nathan EA, Doherty DA, Simmer KN: **Benefits of**  
821 **Bifidobacterium breve M-16V Supplementation in Preterm Neonates - A Retrospective**  
822 **Cohort Study.** *PLoS One* 2016, **11**:e0150775.
- 823 8. Gueimonde M, Margolles A, de los Reyes-Gavilan CG, Salminen S: **Competitive exclusion**  
824 **of enteropathogens from human intestinal mucus by Bifidobacterium strains with**  
825 **acquired resistance to bile--a preliminary study.** *Int J Food Microbiol* 2007, **113**:228-  
826 232.
- 827 9. Lievin V, Peiffer I, Hudault S, Rochat F, Brassart D, Neeser JR, Servin AL: **Bifidobacterium**  
828 **strains from resident infant human gastrointestinal microflora exert antimicrobial**  
829 **activity.** *Gut* 2000, **47**:646-652.
- 830 10. Mennigen R, Nolte K, Rijcken E, Utech M, Loeffler B, Senninger N, Bruewer M: **Probiotic**  
831 **mixture VSL#3 protects the epithelial barrier by maintaining tight junction protein**  
832 **expression and preventing apoptosis in a murine model of colitis.** *Am J Physiol*  
833 *Gastrointest Liver Physiol* 2009, **296**:G1140-1149.
- 834 11. Ewaschuk JB, Diaz H, Meddings L, Diederichs B, Dmytrash A, Backer J, Looijer-van Langen  
835 M, Madsen KL: **Secreted bioactive factors from Bifidobacterium infantis enhance**  
836 **epithelial cell barrier function.** *Am J Physiol Gastrointest Liver Physiol* 2008, **295**:G1025-  
837 1034.
- 838 12. Alessandri G, Ossiprandi MC, MacSharry J, van Sinderen D, Ventura M: **Bifidobacterial**  
839 **Dialogue With Its Human Host and Consequent Modulation of the Immune System.**  
840 *Front Immunol* 2019, **10**:2348.
- 841 13. Fanning S, Hall LJ, Cronin M, Zomer A, MacSharry J, Goulding D, Motherway MO,  
842 Shanahan F, Nally K, Dougan G, van Sinderen D: **Bifidobacterial surface-**  
843 **exopolysaccharide facilitates commensal-host interaction through immune**  
844 **modulation and pathogen protection.** *Proc Natl Acad Sci U S A* 2012, **109**:2108-2113.

- 845 14. Yan F, Polk DB: **Probiotics and immune health.** *Curr Opin Gastroenterol* 2011, **27**:496-  
846 501.
- 847 15. Klaenhammer TR, Kleerebezem M, Kopp MV, Rescigno M: **The impact of probiotics and**  
848 **prebiotics on the immune system.** *Nat Rev Immunol* 2012, **12**:728-734.
- 849 16. Zoetendal EG, Raes J, van den Bogert B, Arumugam M, Booijink CC, Troost FJ, Bork P,  
850 Wels M, de Vos WM, Kleerebezem M: **The human small intestinal microbiota is driven**  
851 **by rapid uptake and conversion of simple carbohydrates.** *ISME J* 2012, **6**:1415-1426.
- 852 17. Bloom PD, Boedeker EC: **Mucosal immune responses to intestinal bacterial pathogens.**  
853 *Semin Gastrointest Dis* 1996, **7**:151-166.
- 854 18. Reid G, Younes JA, Van der Mei HC, Gloor GB, Knight R, Busscher HJ: **Microbiota**  
855 **restoration: natural and supplemented recovery of human microbial communities.** *Nat*  
856 *Rev Microbiol* 2011, **9**:27-38.
- 857 19. Sarkar A, Mandal S: **Bifidobacteria-Insight into clinical outcomes and mechanisms of its**  
858 **probiotic action.** *Microbiol Res* 2016, **192**:159-171.
- 859 20. Geva-Zatorsky N, Sefik E, Kua L, Pasmán L, Tan TG, Ortiz-Lopez A, Yanortsang TB, Yang L,  
860 Jupp R, Mathis D, et al: **Mining the Human Gut Microbiota for Immunomodulatory**  
861 **Organisms.** *Cell* 2017, **168**:928-943 e911.
- 862 21. Dong H, Rowland I, Yaqoob P: **Comparative effects of six probiotic strains on immune**  
863 **function in vitro.** *Br J Nutr* 2012, **108**:459-470.
- 864 22. Medina M, Izquierdo E, Ennahar S, Sanz Y: **Differential immunomodulatory properties**  
865 **of Bifidobacterium logum strains: relevance to probiotic selection and clinical**  
866 **applications.** *Clin Exp Immunol* 2007, **150**:531-538.
- 867 23. Bron PA, van Baarlen P, Kleerebezem M: **Emerging molecular insights into the**  
868 **interaction between probiotics and the host intestinal mucosa.** *Nat Rev Microbiol*  
869 2011, **10**:66-78.
- 870 24. Hoarau C, Martin L, Faugaret D, Baron C, Dauba A, Aubert-Jacquin C, Velge-Roussel F,  
871 Lebranchu Y: **Supernatant from bifidobacterium differentially modulates transduction**  
872 **signaling pathways for biological functions of human dendritic cells.** *PLoS One* 2008,  
873 **3**:e2753.
- 874 25. Wittmann A, Autenrieth IB, Frick JS: **Plasmacytoid dendritic cells are crucial in**  
875 **Bifidobacterium adolescentis-mediated inhibition of Yersinia enterocolitica infection.**  
876 *PLoS One* 2013, **8**:e71338.
- 877 26. van Baarlen P, Troost F, van der Meer C, Hooiveld G, Boekschoten M, Brummer RJ,  
878 Kleerebezem M: **Human mucosal in vivo transcriptome responses to three lactobacilli**  
879 **indicate how probiotics may modulate human cellular pathways.** *Proc Natl Acad Sci U*  
880 *S A* 2011, **108 Suppl 1**:4562-4569.
- 881 27. Turrone F, Serafini F, Foroni E, Duranti S, O'Connell Motherway M, Taverniti V,  
882 Mangifesta M, Milani C, Viappiani A, Roversi T, et al: **Role of sortase-dependent pili of**  
883 **Bifidobacterium bifidum PRL2010 in modulating bacterium-host interactions.** *Proc Natl*  
884 *Acad Sci U S A* 2013, **110**:11151-11156.
- 885 28. Hickey A, Stamou P, Udayan S, Ramon-Vazquez A, Esteban-Torres M, Bottacini F,  
886 Woznicki JA, Hughes O, Melgar S, Ventura M, et al: **Bifidobacterium breve**  
887 **Exopolysaccharide Blocks Dendritic Cell Maturation and Activation of CD4(+) T Cells.**  
888 *Front Microbiol* 2021, **12**:653587.

- 889 29. Grangette C, Nutten S, Palumbo E, Morath S, Hermann C, Dewulf J, Pot B, Hartung T,  
890 Hols P, Mercenier A: **Enhanced antiinflammatory capacity of a *Lactobacillus plantarum***  
891 **mutant synthesizing modified teichoic acids.** *Proc Natl Acad Sci U S A* 2005, **102**:10321-  
892 10326.
- 893 30. Fukuda S, Toh H, Hase K, Oshima K, Nakanishi Y, Yoshimura K, Tobe T, Clarke JM,  
894 Topping DL, Suzuki T, et al: **Bifidobacteria can protect from enteropathogenic infection**  
895 **through production of acetate.** *Nature* 2011, **469**:543-547.
- 896 31. Pineiro M, Stanton C: **Probiotic bacteria: legislative framework-- requirements to**  
897 **evidence basis.** *J Nutr* 2007, **137**:850S-853S.
- 898 32. Daniel C, Poiret S, Goudercourt D, Dennin V, Leyer G, Pot B: **Selecting lactic acid**  
899 **bacteria for their safety and functionality by use of a mouse colitis model.** *Appl Environ*  
900 *Microbiol* 2006, **72**:5799-5805.
- 901 33. Bromberg JS, Hittle LE, Xiong Y, Saxena V, Smyth EM, Li L, Zhang T, Wagner C, Fricke WF,  
902 Simon T, et al: **Gut microbiota-dependent modulation of innate immunity and lymph**  
903 **node remodeling affects cardiac allograft outcomes.** *JCI Insight* 2018, **3**.
- 904 34. Mongodin EF, Hittle LL, Nadendla S, Brinkman CC, Xiong Y, Bromberg JS: **Complete**  
905 **Genome Sequence of a Strain of *Bifidobacterium pseudolongum* Isolated from Mouse**  
906 **Feces and Associated with Improved Organ Transplant Outcome.** *Genome Announc*  
907 2017, **5**.
- 908 35. Lugli GA, Duranti S, Albert K, Mancabelli L, Napoli S, Viappiani A, Anzalone R, Longhi G,  
909 Milani C, Turrone F, et al: **Unveiling Genomic Diversity among Members of the Species**  
910 ***Bifidobacterium pseudolongum*, a Widely Distributed Gut Commensal of the Animal**  
911 **Kingdom.** *Appl Environ Microbiol* 2019, **85**.
- 912 36. Lugli GA, Milani C, Duranti S, Mancabelli L, Mangifesta M, Turrone F, Viappiani A, van  
913 Sinderen D, Ventura M: **Tracking the Taxonomy of the Genus *Bifidobacterium* Based on**  
914 **a Phylogenomic Approach.** *Appl Environ Microbiol* 2018, **84**.
- 915 37. Pokusaeva K, Fitzgerald GF, van Sinderen D: **Carbohydrate metabolism in**  
916 ***Bifidobacteria*.** *Genes Nutr* 2011, **6**:285-306.
- 917 38. Lombard V, Golaconda Ramulu H, Drula E, Coutinho PM, Henrissat B: **The carbohydrate-**  
918 **active enzymes database (CAZy) in 2013.** *Nucleic Acids Res* 2014, **42**:D490-495.
- 919 39. Milani C, Lugli GA, Duranti S, Turrone F, Mancabelli L, Ferrario C, Mangifesta M, Hevia A,  
920 Viappiani A, Scholz M, et al: **Bifidobacteria exhibit social behavior through**  
921 **carbohydrate resource sharing in the gut.** *Sci Rep* 2015, **5**:15782.
- 922 40. van Wely KH, Swaving J, Freudl R, Driessen AJ: **Translocation of proteins across the cell**  
923 **envelope of Gram-positive bacteria.** *FEMS Microbiol Rev* 2001, **25**:437-454.
- 924 41. Lugli GA, Mancino W, Milani C, Duranti S, Turrone F, van Sinderen D, Ventura M:  
925 **Reconstruction of the Bifidobacterial Pan-Secretome Reveals the Network of**  
926 **Extracellular Interactions between Bifidobacteria and the Infant Gut.** *Appl Environ*  
927 *Microbiol* 2018, **84**.
- 928 42. Osswald A, Westermann C, Sun Z, Riedel CU: **A Phytase-Based Reporter System for**  
929 **Identification of Functional Secretion Signals in Bifidobacteria.** *PLoS One* 2015,  
930 **10**:e0128802.
- 931 43. Artis D: **Epithelial-cell recognition of commensal bacteria and maintenance of immune**  
932 **homeostasis in the gut.** *Nat Rev Immunol* 2008, **8**:411-420.

- 933 44. Chen X, Katchar K, Goldsmith JD, Nanthakumar N, Cheknis A, Gerding DN, Kelly CP: **A**  
934 **mouse model of Clostridium difficile-associated disease.** *Gastroenterology* 2008,  
935 **135:1984-1992.**
- 936 45. Warren KJ, Iwami D, Harris DG, Bromberg JS, Burrell BE: **Laminins affect T cell trafficking**  
937 **and allograft fate.** *J Clin Invest* 2014, **124:2204-2218.**
- 938 46. Li L, Shirkey MW, Zhang T, Xiong Y, Piao W, Saxena V, Paluskievicz C, Lee Y, Toney N,  
939 Cerel BM, et al: **The lymph node stromal laminin alpha5 shapes alloimmunity.** *J Clin*  
940 *Invest* 2020, **130:2602-2619.**
- 941 47. Kieser S, Zdobnov EM, Trajkovski M: **Comprehensive mouse gut metagenome catalog**  
942 **reveals major difference to the human counterpart.** *bioRxiv*  
943 2021:2021.2003.2018.435958.
- 944 48. Segata N, Izard J, Waldron L, Gevers D, Miropolsky L, Garrett WS, Huttenhower C:  
945 **Metagenomic biomarker discovery and explanation.** *Genome biology* 2011, **12:R60.**
- 946 49. Centanni M, Lawley B, Butts CA, Roy NC, Lee J, Kelly WJ, Tannock GW: **Bifidobacterium**  
947 **pseudolongum in the Ceca of Rats Fed Hi-Maize Starch Has Characteristics of a**  
948 **Keystone Species in Bifidobacterial Blooms.** *Appl Environ Microbiol* 2018, **84.**
- 949 50. Odamaki T, Kato K, Sugahara H, Xiao JZ, Abe F, Benno Y: **Effect of probiotic yoghurt on**  
950 **animal-based diet-induced change in gut microbiota: an open, randomised, parallel-**  
951 **group study.** *Benef Microbes* 2016, **7:473-484.**
- 952 51. Odamaki T, Sugahara H, Yonezawa S, Yaeshima T, Iwatsuki K, Tanabe S, Tominaga T,  
953 Togashi H, Benno Y, Xiao JZ: **Effect of the oral intake of yogurt containing**  
954 **Bifidobacterium longum BB536 on the cell numbers of enterotoxigenic Bacteroides**  
955 **fragilis in microbiota.** *Anaerobe* 2012, **18:14-18.**
- 956 52. Toscano M, De Grandi R, Stronati L, De Vecchi E, Drago L: **Effect of Lactobacillus**  
957 **rhamnosus HN001 and Bifidobacterium longum BB536 on the healthy gut microbiota**  
958 **composition at phyla and species level: A preliminary study.** *World J Gastroenterol*  
959 2017, **23:2696-2704.**
- 960 53. Ding S, Yan W, Ma Y, Fang J: **The impact of probiotics on gut health via alternation of**  
961 **immune status of monogastric animals.** *Anim Nutr* 2021, **7:24-30.**
- 962 54. Maldonado-Gomez MX, Martinez I, Bottacini F, O'Callaghan A, Ventura M, van Sinderen  
963 D, Hillmann B, Vangay P, Knights D, Hutkins RW, Walter J: **Stable Engraftment of**  
964 **Bifidobacterium longum AH1206 in the Human Gut Depends on Individualized**  
965 **Features of the Resident Microbiome.** *Cell Host Microbe* 2016, **20:515-526.**
- 966 55. Sorbara MT, Pamer EG: **Interbacterial mechanisms of colonization resistance and the**  
967 **strategies pathogens use to overcome them.** *Mucosal Immunol* 2019, **12:1-9.**
- 968 56. Chiu L, Bazin T, Truchetet ME, Schaeferbeke T, Delhaes L, Pradeu T: **Protective**  
969 **Microbiota: From Localized to Long-Reaching Co-Immunity.** *Front Immunol* 2017,  
970 **8:1678.**
- 971 57. El Kaoutari A, Armougom F, Gordon JI, Raoult D, Henrissat B: **The abundance and**  
972 **variety of carbohydrate-active enzymes in the human gut microbiota.** *Nat Rev*  
973 *Microbiol* 2013, **11:497-504.**
- 974 58. Odamaki T, Horigome A, Sugahara H, Hashikura N, Minami J, Xiao JZ, Abe F:  
975 **Comparative Genomics Revealed Genetic Diversity and Species/Strain-Level**

- 976 **Differences in Carbohydrate Metabolism of Three Probiotic Bifidobacterial Species.** *Int*  
977 *J Genomics* 2015, **2015**:567809.
- 978 59. Yang C, Mogno I, Contijoch EJ, Borgerding JN, Aggarwala V, Li Z, Siu S, Grasset EK,  
979 Helmus DS, Dubinsky MC, et al: **Fecal IgA Levels Are Determined by Strain-Level**  
980 **Differences in Bacteroides ovatus and Are Modifiable by Gut Microbiota**  
981 **Manipulation.** *Cell Host Microbe* 2020, **27**:467-475 e466.
- 982 60. Kukkonen K, Kuitunen M, Haahtela T, Korpela R, Poussa T, Savilahti E: **High intestinal IgA**  
983 **associates with reduced risk of IgE-associated allergic diseases.** *Pediatr Allergy*  
984 *Immunol* 2010, **21**:67-73.
- 985 61. Yoshida Y, Seki T, Matsunaka H, Watanabe T, Shindo M, Yamada N, Yamamoto O:  
986 **Clinical effects of probiotic bifidobacterium breve supplementation in adult patients**  
987 **with atopic dermatitis.** *Yonago Acta Med* 2010, **53**:37-45.
- 988 62. Zhang CY, Chen GF, Wang YY, Xu Z, Wang YG, Song XL: **peptidoglycan extracted from**  
989 **Bifidobacterium sp. could enhance immunological ability of Apostichopus japonicus.**  
990 *Aquac Nutr* 2015, **21**:679-689.
- 991 63. Abbad Andaloussi S, Talbaoui H, Marczak R, Bonaly R: **Isolation and characterization of**  
992 **exocellular polysaccharides produced by Bifidobacterium longum.** *Appl Microbiol*  
993 *Biotechnol* 1995, **43**:995-1000.
- 994 64. Bromberg JS, Hittle L, Xiong Y, Saxena V, Smyth EM, Li L, Zhang T, Wagner C, Fricke WF,  
995 Simon T, et al: **Gut microbiota-dependent modulation of innate immunity and lymph**  
996 **node remodeling affects cardiac allograft outcomes.** *JCI Insight* 2018, **3**.
- 997 65. Nurk S, Bankevich A, Antipov D, Gurevich AA, Korobeynikov A, Lapidus A, Prjibelski AD,  
998 Pyskhin A, Sirotkin A, Sirotkin Y, et al: **Assembling single-cell genomes and mini-**  
999 **metagenomes from chimeric MDA products.** *J Comput Biol* 2013, **20**:714-737.
- 1000 66. Rissman AI, Mau B, Biehl BS, Darling AE, Glasner JD, Perna NT: **Reordering contigs of**  
1001 **draft genomes using the Mauve aligner.** *Bioinformatics* 2009, **25**:2071-2073.
- 1002 67. Darling AE, Mau B, Perna NT: **progressiveMauve: multiple genome alignment with gene**  
1003 **gain, loss and rearrangement.** *PloS one* 2010, **5**:e11147.
- 1004 68. Bajpai V, Majumder R, Rather I, Kim K: **Extraction, isolation and purification of**  
1005 **exopolysaccharide from lactic acid bacteria using ethanol precipitation method.**  
1006 *Bangladesh Journal of Pharmacology* 2016, **11**:573-576.
- 1007 69. Delmont TO, Eren AM: **Linking pangenomes and metagenomes: the Prochlorococcus**  
1008 **metapangenome.** *PeerJ* 2018, **6**:e4320.
- 1009 70. **An anvio workflow for microbial pangenomics**  
1010 [<http://merenlab.org/2016/11/08/pangenomics-v2/>]
- 1011 71. Pierce NT, Irber L, Reiter T, Brooks P, Brown CT: **Large-scale sequence comparisons with**  
1012 **sourmash.** *F1000Res* 2019, **8**:1006.
- 1013 72. Enright AJ, Van Dongen S, Ouzounis CA: **An efficient algorithm for large-scale detection**  
1014 **of protein families.** *Nucleic Acids Res* 2002, **30**:1575-1584.
- 1015 73. Edgar RC: **MUSCLE: multiple sequence alignment with high accuracy and high**  
1016 **throughput.** *Nucleic Acids Res* 2004, **32**:1792-1797.
- 1017 74. Huerta-Cepas J, Szklarczyk D, Heller D, Hernandez-Plaza A, Forslund SK, Cook H, Mende  
1018 DR, Letunic I, Rattei T, Jensen LJ, et al: **eggNOG 5.0: a hierarchical, functionally and**

- 1019 **phylogenetically annotated orthology resource based on 5090 organisms and 2502**  
1020 **viruses. *Nucleic Acids Res* 2019, **47**:D309-D314.**
- 1021 75. Huerta-Cepas J, Forslund K, Pedro Coelho L, Szklarczyk D, Juhl Jensen L, von Mering C,  
1022 Bork P: **Fast genome-wide functional annotation through orthology assignment by**  
1023 **eggNOG-mapper. *Mol Biol Evol* 2017.**
- 1024 76. Mistry J, Chuguransky S, Williams L, Qureshi M, Salazar GA, Sonnhammer ELL, Tosatto  
1025 SCE, Paladin L, Raj S, Richardson LJ, et al: **Pfam: The protein families database in 2021.**  
1026 ***Nucleic Acids Res* 2021, **49**:D412-D419.**
- 1027 77. Kanehisa M, Sato Y, Kawashima M, Furumichi M, Tanabe M: **KEGG as a reference**  
1028 **resource for gene and protein annotation. *Nucleic Acids Res* 2016, **44**:D457-462.**
- 1029 78. Kanehisa M, Sato Y, Morishima K: **BlastKOALA and GhostKOALA: KEGG Tools for**  
1030 **Functional Characterization of Genome and Metagenome Sequences. *J Mol Biol* 2016,**  
1031 ****428**:726-731.**
- 1032 79. Storey JD, Tibshirani R: **Statistical significance for genomewide studies. *Proc Natl Acad***  
1033 ***Sci U S A* 2003, **100**:9440-9445.**
- 1034 80. Zhang H, Yohe T, Huang L, Entwistle S, Wu P, Yang Z, Busk PK, Xu Y, Yin Y: **dbCAN2: a**  
1035 **meta server for automated carbohydrate-active enzyme annotation. *Nucleic Acids Res***  
1036 **2018, **46**:W95-W101.**
- 1037 81. Yu NY, Wagner JR, Laird MR, Melli G, Rey S, Lo R, Dao P, Sahinalp SC, Ester M, Foster LJ,  
1038 Brinkman FS: **PSORTb 3.0: improved protein subcellular localization prediction with**  
1039 **refined localization subcategories and predictive capabilities for all prokaryotes.**  
1040 ***Bioinformatics* 2010, **26**:1608-1615.**
- 1041 82. Piao W, Xiong Y, Li L, Saxena V, Smith KD, Hippen KL, Paluskiewicz C, Willsonshirkey M,  
1042 Blazar BR, Abdi R, Bromberg JS: **Regulatory T Cells Condition Lymphatic Endothelia for**  
1043 **Enhanced Transendothelial Migration. *Cell Rep* 2020, **30**:1052-1062 e1055.**
- 1044 83. Rotmistrovsky K, Agarwala R: **BMTagger: Best Match Tagger for removing human reads**  
1045 **from metagenomics datasets. NCBI/NLM, National Institutes of Health; 2011.**
- 1046 84. Church DM, Schneider VA, Graves T, Auger K, Cunningham F, Bouk N, Chen HC, Agarwala  
1047 R, McLaren WM, Ritchie GR, et al: **Modernizing reference genome assemblies. *PLoS***  
1048 ***biology* 2011, **9**:e1001091.**
- 1049 85. Chen S, Zhou Y, Chen Y, Gu J: **fastp: an ultra-fast all-in-one FASTQ preprocessor.**  
1050 ***Bioinformatics* 2018, **34**:i884-i890.**
- 1051 86. Wood DE, Lu J, Langmead B: **Improved metagenomic analysis with Kraken 2. *Genome***  
1052 ***Biol* 2019, **20**:257.**
- 1053 87. Lu J, Breitwieser FP, Thielen P, SL S: **Bracken: estimating species abundance in**  
1054 **metagenomics data. *PeerJ Computer Science* 2017, **3**:e104.**
- 1055 88. McMurdie PJ, Holmes S: **phyloseq: an R package for reproducible interactive analysis**  
1056 **and graphics of microbiome census data. *PLoS One* 2013, **8**:e61217.**
- 1057 89. Fisher RA: **The use of multiple measurements in taxonomic problems. *Ann Eugenics***  
1058 **1936, **7**.**
- 1059 90. Kanehisa M, Goto S, Sato Y, Furumichi M, Tanabe M: **KEGG for integration and**  
1060 **interpretation of large-scale molecular data sets. *Nucleic acids research* 2012, **40**:D109-**  
1061 **114.**

- 1062 91. Franzosa EA, McIver LJ, Rahnavard G, Thompson LR, Schirmer M, Weingart G, Lipson KS,  
1063 Knight R, Caporaso JG, Segata N, Huttenhower C: **Species-level functional profiling of**  
1064 **metagenomes and metatranscriptomes.** *Nat Methods* 2018, **15**:962-968.
- 1065 92. Jari Oksanen FGB, Michael Friendly, Roeland Kindt, Pierre Legendre, Dan McGlinn, Peter  
1066 R. Minchin, R. B. O'Hara, Gavin L. Simpson, Peter Solymos, M. Henry H. Stevens, Eduard  
1067 Szoecs and Helene Wagner **vegan: Community Ecology Package. R package.** version 2.4-  
1068 1. edition; 2016.
- 1069 93. Dixon P: **VEGAN, a package of R functions for community ecology.** *Journal of*  
1070 *Vegetation Science* 2003, **14**:927-930.
- 1071 94. Oksanen J, Blanchet FG, Kindt R, Legendre P, Minchin PR, O'Hara RB, Simpson GL,  
1072 Solymos P, Stevens MHH, Wagner H: **vegan: Community Ecology Package. R package**  
1073 **version 2.0-2** 2011.
- 1074 95. Gorokhova E: **Effects of preservation and storage of microcrustaceans in RNAlater on**  
1075 **RNA and DNA degradation.** . *Limnol Oceanogr: Methods* 2005, **3**:143-148.
- 1076 96. Kim D, Langmead B, Salzberg SL: **HISAT: a fast spliced aligner with low memory**  
1077 **requirements.** *Nat Methods* 2015, **12**:357-360.
- 1078 97. Anders S, Pyl PT, Huber W: **HTSeq--a Python framework to work with high-throughput**  
1079 **sequencing data.** *Bioinformatics* 2015, **31**:166-169.
- 1080 98. Anders S, Huber W: **Differential expression analysis for sequence count data.** *Genome*  
1081 *Biol* 2010, **11**:R106.
- 1082 99. Boyle EI, Weng S, Gollub J, Botstein D, Cherry JM, Sherlock G: **GO::TermFinder—open**  
1083 **source software for accessing Gene Ontology information and finding significantly**  
1084 **enriched Gene Ontology terms associated with a list of genes.** *Bioinformatics* 2014,  
1085 **20**:3710-3715.
- 1086 100. G Y, L W, Y H, Q H: **clusterProfiler: an R package for comparing biological themes**  
1087 **among gene clusters.** *OMICS: A Journal of Integrative Biology* 2012, **16**:284-287.  
1088

1089 **Ethical Approval and Consent to participate**

1090 All animal studies were carried out in accordance with IACUC-approved protocols.

1091 **Consent for publication**

1092 Not applicable

1093 **Availability of data and materials**

1094 The assembly of the genomes (accession numbers were listed in Supplemental Table  
1095 2), metagenome (SRP361281), and transcriptome sequences were submitted to  
1096 GenBank under BioProject PRJNA809764.

1097 **Competing interests**

1098 The authors declare no competing financial and non-financial interests.

1099 **Funding**

1100 This work was supported by National Institute of Health (NIH) National Heart, Lung and  
1101 Blood Institute award R01HL148672 (JSB/BM) and NIH National Institute of Allergy and  
1102 Infectious Diseases training grant T32AI95190-10 (SJG).

1103 **Authors' contributions**

1104 B. M., E. F. M, J. B. designed the experiments. S. J. G., V. S., W. P., R. L., L. L., C. P.,  
1105 M.W. conducted and analyzed the *in vitro* and *in vivo* experiments. H. W. L. performed  
1106 the AN Biolog assay and RNA extraction. L. H., E. F. M., A. M. performed colony  
1107 isolation and strain characterization. B. M. and Y. S. performed the bioinformatics  
1108 analyses. B. M., M. F. performed the statistical analyses. B. M., S. J. G., M. F., E. F. M.,  
1109 and J. S. B. wrote the manuscript. B. M., J. S. B. are co-corresponding authors for this  
1110 manuscript.

1111 **Acknowledgements**

1112 This manuscript has been released as a pre-print at BioRxiv MS ID#:  
1113 BIORXIV/2022/484607. The authors thank C. Colin Brinkman and Yanbao Xiong at the  
1114 University of Maryland for helping with pilot data and initial experiment preparation.  
1115 Emmanuel Mongodin, PhD, contributed to this work as an employee of the University of  
1116 Maryland School of Medicine. The views expressed in this manuscript are his own and  
1117 do not necessarily represent the views of the National Institutes of Health or the United  
1118 States Government.

1119 **Authors' information**

1120 Not applicable

1121

1122 **Figures**

1123 **Figure 1. Pangenome analyses of *B. pseudolongum* genomes.** Pangenome  
1124 constructed using 79 strains, including the 5 strains sequenced in this study  
1125 (**Supplemental Table 3**) and displayed using *anvi'o vers* 6.2 [69]. Homologous gene  
1126 clusters (HGCs) were identified based on all-versus-all sequence similarity in left panel  
1127 and categorized as core, accessory or dispensable depending on their level of  
1128 conservation. Genome ANI (Average Nucleotide Identity) was calculated using  
1129 Sourmash vers 3.3 [71]. Blue arrows indicate the two strains compared: ATCC25526  
1130 and UMB-MBP-001. Black arrows indicate the other three *B. pseudolongum* strains  
1131 isolated from the source stool of pregnant mice.

1132

1133 **Figure 2. *Bifidobacterium* alters DC and MΦ surface phenotype.** DC and MΦ  
1134 cultured with media alone, ATCC25526 (ATCC) or UMB-MBP-01 (MD) UV-killed  
1135 *Bifidobacterium* or EPS derived from each strain. After 24 hrs of culture, cells analyzed  
1136 by flow cytometry. DC gated on live CD11c+, and MΦ gated on live F4/80+ populations.  
1137 DC stained for **A)** MHC class II, **B)** CD40, **C)** CD80, and **D)** CD86. MΦ stained for **E)**  
1138 MHC class II, **F)** CD40 and **G)** CD80. MFI: mean fluorescence intensity; DC: Bone  
1139 marrow derived dendritic cells; MΦ: peritoneal macrophages; MFI values normalized to  
1140 control and compared using one-way ANOVA. \* p value < 0.05; \*\* p value < 0.01. MΦ  
1141 data representative of two experiments. DC data represented as merge of one  
1142 experiment with EPS and one experiment with UV killed bacteria, each data set is  
1143 normalized to its respective control.

1144

1145 **Figure 3. *Bifidobacterium* alters DC and M $\Phi$  cytokine secretion.** DCs (**A-C**) or M $\Phi$   
1146 (**D-F**) stimulated with EPS or UV-killed ATCC25526 (ATCC) or UMB-MBP-01 (MD), and  
1147 24 hrs later supernatants analyzed for **A, D**) IL-6, **B, E**) TNF $\alpha$ , and **C, F**) IL-10 by  
1148 ELISA. Treatments compared using one-way ANOVA. \* p value < 0.05; \*\* p value <  
1149 0.01, \*\*\* p value < 0.001, \*\*\*\* p value < 0.0001. Data representative of two separate  
1150 experiments.

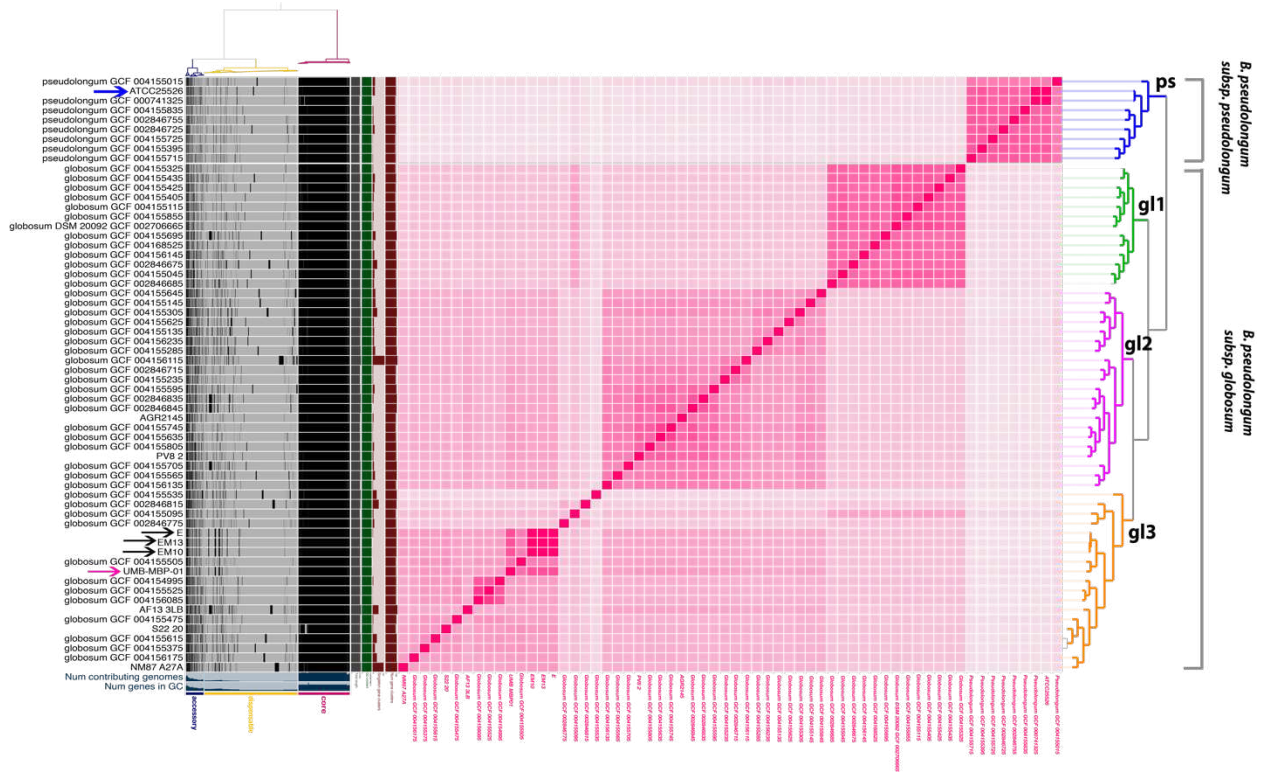
1151  
1152 **Figure 4. *Bifidobacterium* strains induce unique changes in local and systemic**  
1153 **immune cell distribution and LN architecture. A)** Experimental design. C57BL/6  
1154 mice treated with antibiotics for 6 days followed by gavage with *B. pseudolongum*  
1155 ATCC25526 (ATCC), UMB-MBP-01 (MD), or PBS (control). Mice then treated with the  
1156 immunosuppressant tacrolimus for the next two days. Tissues harvested 2 days after  
1157 FMT. Frozen sections of small intestine stained for **B**) Treg (anti-Foxp3 mAb), and **C**)  
1158 DC (anti-CD11c mAb). MLN sections stained for **D**) DC (anti-CD11c mAb) and **E**)  
1159 M $\Phi$  (anti-F4/80 mAb). LN stained for laminin  $\alpha$ 4 and laminin  $\alpha$ 5 and laminin  $\alpha$ 4: $\alpha$ 5 ratio  
1160 calculated for **F**) MLN CR, and **G**) PLN CR. MFI: mean fluorescence intensity. MLN:  
1161 mesenteric lymph nodes; PLN: peripheral lymph node. MFI values normalized using the  
1162 sum of mean, and categories compared using one-way ANOVA. \* p value < 0.05; \*\* p  
1163 value < 0.01, \*\*\* p value < 0.001, \*\*\*\* p value < 0.0001. Data representative of two  
1164 separate experiments, 3 mice/group.

1165  
1166 **Figure 5. Transcriptome profiling of intestinal tissues in response to ATCC25526**  
1167 **or UMB-MBP-01. A)** Quadrant plot to show whether differential expressed genes

1168 (DEGs) have the same or opposite relationships between each of the pairwise  
1169 comparison of UMB-MBP-001 vs control and UMB-MBP-001 vs ATCC25526. DEGs  
1170 were determined using log<sub>2</sub> fold change (LFC) >(±)1 and false discovery rate  
1171 (FDR)<0.05. **B)** Gene-Concept network for most over-represented Gene Ontology (GO)  
1172 terms to depict over-represented functions based on q-value and gene-count. Over-  
1173 representation analyses [99] of DEGs that are only different abundant in UMB-MBP-001  
1174 vs control but not in ATCC25526 vs control, using GO ontologies performed using  
1175 enrichGO function of clusterProfile Bioconductor package[100]. For pairwise  
1176 comparison enrichment analyses for any two conditions, please refer to **Supplemental**  
1177 **Figure 4.**

1178  
1179 **Figure 6. Alterations in gut microbiome after bacterial engraftment. A)** Heatmap of  
1180 the top 20 most abundant intestinal bacterial taxa relative abundance in mice  
1181 intraluminal samples. Ward linkage clustering based on Jensen-Shannon distance was  
1182 calculated using the vegan package in R [94]. Taxonomic profiles of the microbial  
1183 community were characterized using the comprehensive mouse gut metagenome  
1184 (CMGM) catalog[47]. **B)** Cumulative abundance of major bacterial families. The relative  
1185 abundances of each family are stacked in order from greatest to least, and are  
1186 separated by a horizontal line. **C)** Shannon diversity index (within-community diversity)  
1187 of the four experimental groups. **D), E)** Canonical Correspondence Analysis (CCA) of  
1188 microbial functional pathways characterized using HUMAnN2 (v0.11.2)[91] and Uniref90  
1189 database [90] based on Bray-Curtis distance. CA1 and CA2 selected as the major  
1190 components based on the eigenvalue.

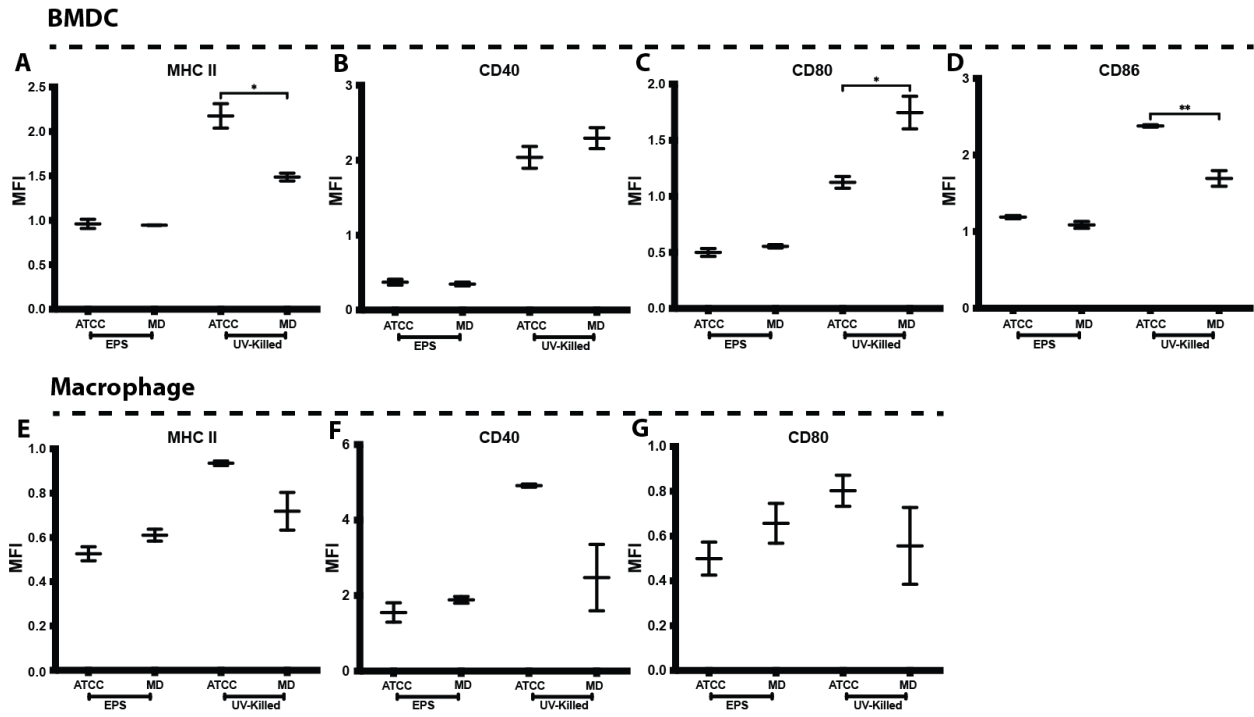
1191 **Figure 1**



1192

1193

1194 **Figure 2**

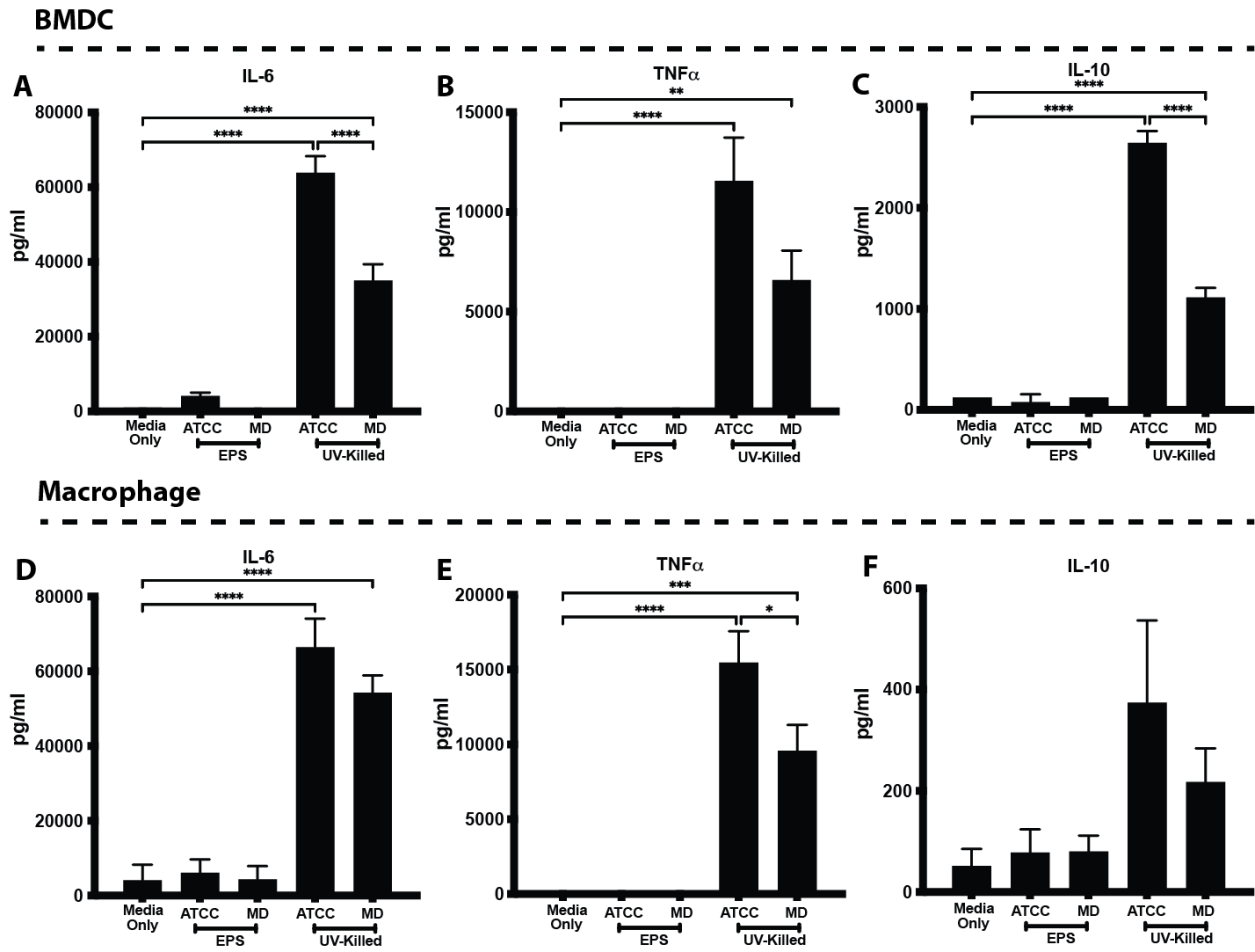


1195

1196

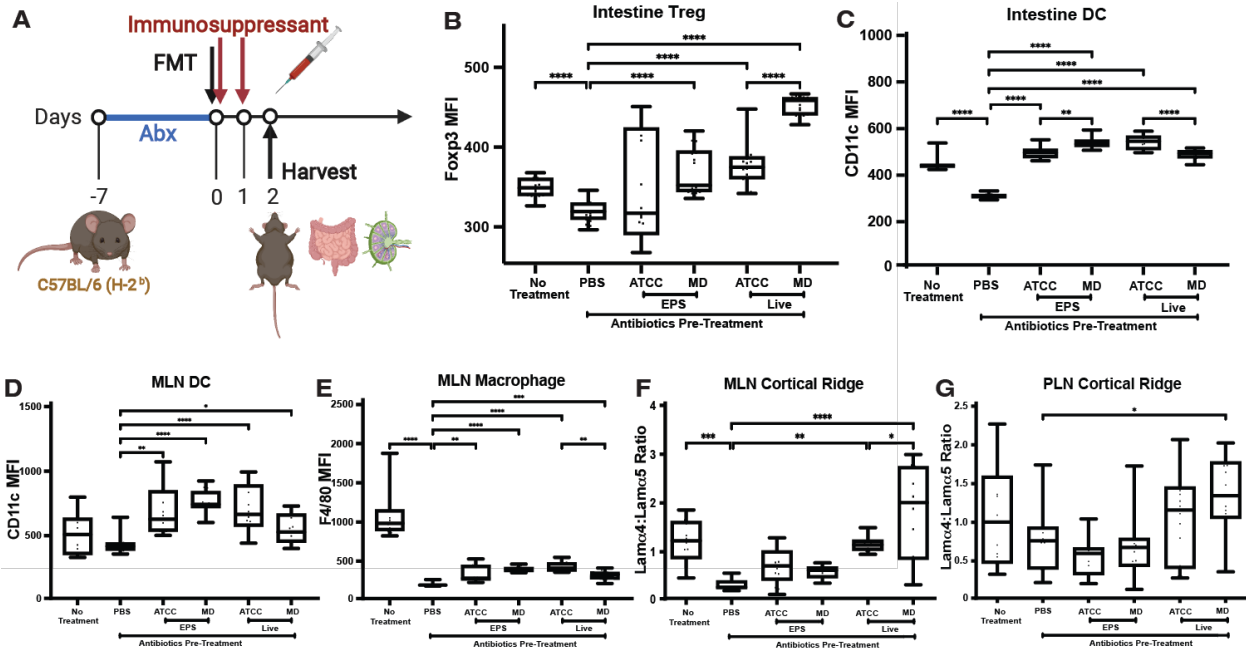
1197 **Figure 3**

1198



1199

1200 **Figure 4**



1201

1202

1203

1204

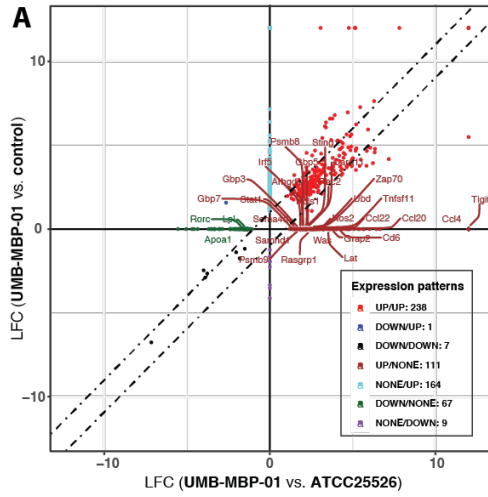
1205

1206

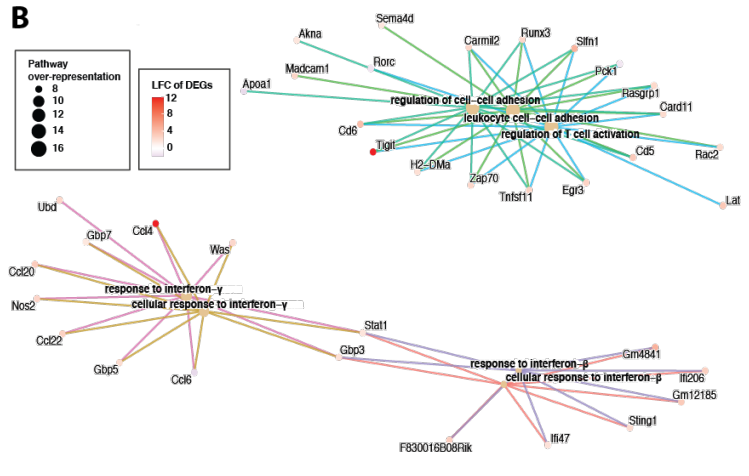
1207

1208 **Figure 5.**

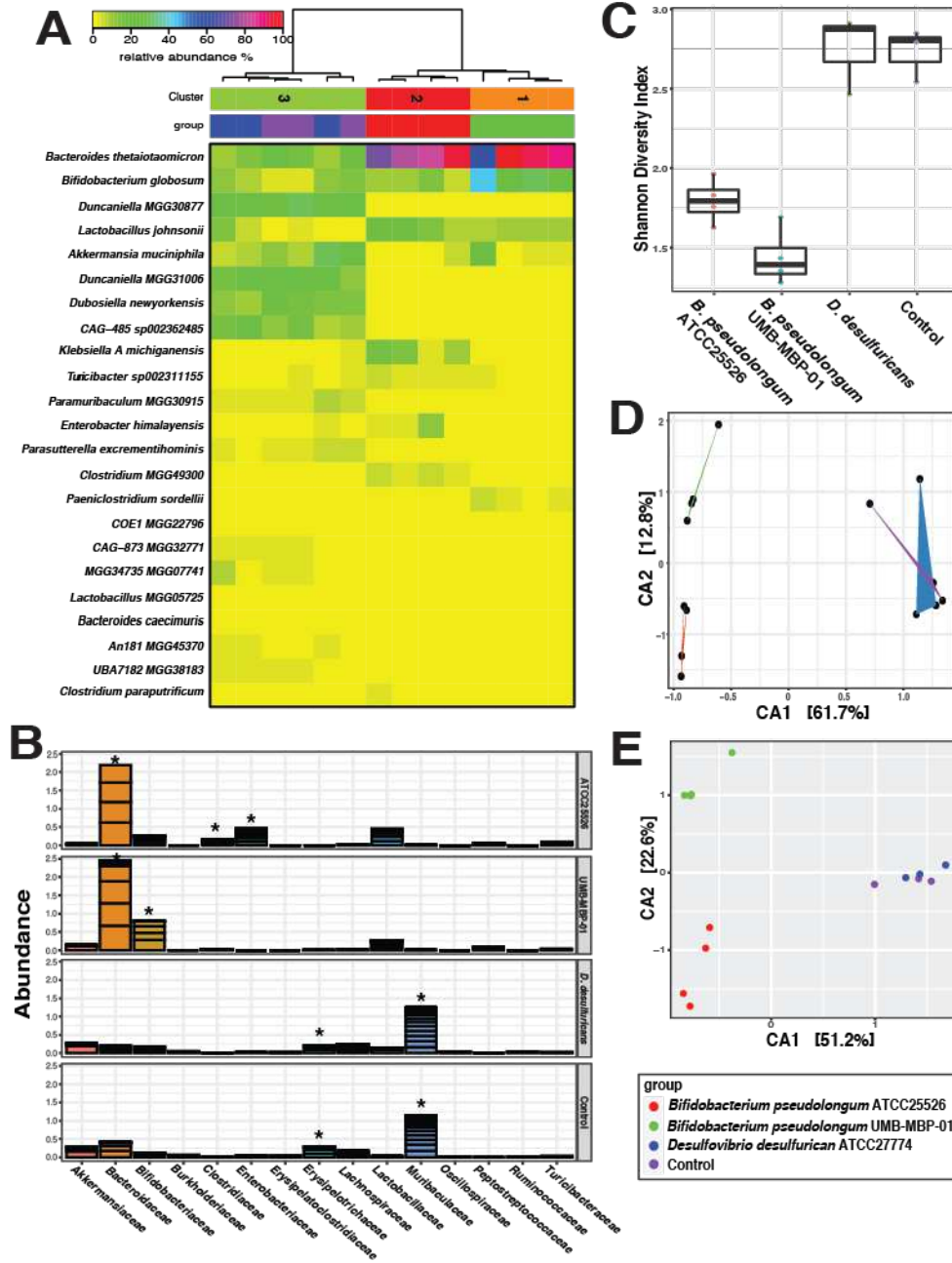
1209



1210



1211 Figure 6.  
1212



1213

## Supplementary Files

This is a list of supplementary files associated with this preprint. Click to download.

- [STable1pangenome.xlsx](#)
- [STable2Sequencingstats.xlsx](#)
- [STable3Biolog.xlsx](#)
- [STable4glycobiome.xlsx](#)
- [STable5localization.xlsx](#)
- [STable6DEGs.xlsx](#)
- [STable7taxonomyMG.xlsx](#)
- [STable8CCA.xlsx](#)
- [STable9GenomeSupplementalAb.docx](#)
- [SupplementalFigures.docx](#)